Supplemental Figure Legends

Figure S1. Creation and characterization of isogenic AML cell lines with RUNX1 R174* mutation. A. DNA electropherogram of OCI-AML2 cells with heterozygous RUNX1 R174* mutation. Sanger sequencing of DNA amplicons cloned in *E. coli* was used to confirm presence of both wild-type and mutant RUNX1 sequence. **B.** DNA electropherogram of HL-60 cells with homozygous RUNX1 R174* mutation. Sanger sequencing of DNA amplicons cloned in *E. coli* was used to confirm presence of biallelic mutant RUNX1 sequence. **C-D**. OCI-AML2, OCI-AML2 RUNX1 R174*/wt, HL-60 and HL-60 RUNX1 R174*/R174* cells were harvested, and total cell lysates were prepared. Immunoblot analyses were conducted for RUNX1 utilizing an N-terminal specific antibody. The expression levels of GAPDH in the lysates served as the loading control. Arrows indicate the positions of full length RUNX1 and truncated RUNX1. **E.** Relative protein expression of RUNX1, PU.1, c-Myc and BIM in OCI-AML2 RUNX1$^{R174*/wt}$ compared to OCI-AML2 control cells. Columns; mean of three experiments $\pm$ S.E.M. * = values significantly different ($p < 0.05$ by two-tailed, unpaired t-test) in OCI-AML2 RUNX1$^{R174*/wt}$ compared to OCI-AML2 control cells. **F**. HL-60 and HL-60 RUNX1 R174*/R174* cells were treated with DMSO (final concentration, 1.2%) for 96 hours. Morphologic differentiation was assessed by light microscopy on cytospun cells stained with hematoxylin and eosin.

Figure S2. Compared to parental OCI-AML2 cells, heterozygous RUNX1 R174* mutation alters the polysome profile, depletes mRNA expression of Myc target genes, ribosomal genes and 5S rRNA levels. A. Total RNA (mRNA + rRNA) quantification in equivalent numbers of OCI-AML2 RUNX1$^{R174*/wt}$ and OCI-AML2 cells. Columns; mean of three experiments $\pm$ S.E.M. n.s. =values not significantly different. **B**. Relative expression of 5S, 5.8S, 18S and 28S rRNA in OCI-AML2 RUNX1$^{R174*/wt}$ and OCI-AML2 cells. Expression normalized to Actin. Columns; mean of three experiments $\pm$ S.E.M. (* = $p < 0.05$; by two-tailed, unpaired t-test). **C-D**. GSEA plots for OCI-AML2 RUNX1$^{R174*/wt}$ cell mRNA expressions compared to HALLMARK Myc Targets I and Myc Targets II pathways. FDR q-values are < 0.1. **E**. GSEA plot for OCI-AML2 RUNX1$^{R174*/wt}$ cell mRNA expressions compared to REACTOME: Signaling by SCF & KIT pathway. **F**. GSEA plot for OCI-AML2 RUNX1$^{R174*/wt}$ cell mRNA expressions compared to HALLMARK: TNFα signaling via NFkB pathway. FDR q-values are < 0.1. **G.** Percent area under the curve in the 40S, 60S, 80S and polysome fraction of OCI-AML2 RUNX1 R174*/wt relative to OCI-AML2 cells. **H**. Ribo-Lace analysis was performed on OCI-AML2 and OCI-AML2 RUNX1$^{R174*/wt}$ cells. Heatmap shows the number of actively translated mRNAs induced and depleted in RUNX1$^{R174*/wt}$ cells compared to parental OCI-AML2 cells. **I**. GSEA plot for OCI-AML2 RUNX1$^{R174*/wt}$ actively translated mRNA expressions compared to GO: Ribosome pathway. FDR q-value < 0.1.

Figure S3. Treatment with homoharringtonine (HHT) is associated with depletion of transcription factor and BCL2 family protein levels but induction of p-JNK signaling. A-B. OCI-AML2 and OCI-AML2 RUNX1$^{R174*/wt}$ cells were treated with the indicated concentrations of homoharringtonine (HHT) for 2-48 hours. Following this, the % of annexin V-positive, apoptotic cells were determined by flow cytometry. Mean of three independent experiments $\pm$ S.E.M. * = $p< 0.05$ as determined by a two-tailed, unpaired t-test. **C**. Densitometry analysis of protein expression changes due to treatment with HHT relative to the untreated control cells. * indicates protein expression alteration values that are significantly different ($p < 0.05$) in OCI-AML2 RUNX1$^{R174*/wt}$ cells treated with HHT compared to the untreated control cells. **D**. Representative immunoblot analysis of OCI-AML2 RUNX1$^{R174*/wt}$ cells treated with HHT as indicated for 8 hours. **E**. OCI-AML2

RUNX1$^{R174*/wt}$ cells were treated with the indicated concentrations of HHT for 2 hours. Total cell lysates were collected and immunoblot analyses were conducted. The expression levels of β-Actin in the cell lysates served as the loading control. **F**. Oncoplot of next generation sequencing (NGS)-detected mutations in cultured AML cell lines harboring RUNX1 mutations. RUNX1 nucleotide mutation, resulting protein change in OCI-AML5 and Mono-Mac-1 cells are shown. **G**. Response of PD mtRUNX1 (n=9) and wt RUNX1 AML (n=14) compared to normal CD34+ HPCs (n=4). Significance was calculated with a two-tailed, unpaired t-test in GraphPad V8. **H**. Expression of tRNA-associated genes in OCI-AML2 RUNX1$^{R174*/wt}$ cells treated with 100 nM of HHT for 8 hours as determined by qPCR analysis utilizing a TaqMan® Array Human Transcription of tRNA assay. Values shown are relative to the expression in untreated OCI-AML2 RUNX1$^{R174*/wt}$ cells. **I**. OCI-AML2 RUNX1$^{R174*/wt}$ cells were treated with the indicated concentrations of HHT or cycloheximide for 4 hours. Nascent polypeptide elongation was detected by OPP puromycin incorporation assay and flow cytometry. **J**-**K**. OCI-AML2, OCI-AML2 RUNX1$^{R174*/wt}$ and OCI-AML5 cells were treated with the indicated concentrations of Rocaglamide for 48 hours. Following this, the % of annexin V-positive, apoptotic cells were determined by flow cytometry. Mean of three independent experiments $\pm$ S.E.M. * = $p < 0.05$ as determined by a two-tailed, unpaired t-test. **L**. Densitometry analysis of protein expression changes due to treatment with venetoclax relative to the untreated control cells. * indicates protein expression alteration values that are significantly different ($p < 0.05$) in OCI-AML2 RUNX1$^{R174*/wt}$ cells treated with venetoclax compared to the untreated control cells. OCI-AML2 and OCI-AML2 RUNX1$^{R174*/wt}$ cells were treated with the indicated concentrations of venetoclax (Ven) for 16 hours. At the end of treatment, cells were fixed and incubated with anti-BAK (NT) [conformation-specific] antibody followed by incubation with a fluorophore conjugated anti-rabbit secondary antibody. Cells were analyzed by flow cytometry. The mean fluorescent intensity of staining is shown. * indicates values that are significantly greater ($p < 0.05$) in OCI-AML2 RUNX1 R174*/wt cells compared to OCI-AML2 cells.

Figure S4. Treatment with HHT alters transcription factor binding site accessibility on chromatin in AML cells. A. Chromatin accessibility in OCI-AML2 and OCI-AML2 RUNX1$^{R174*/wt}$ cells treated with 100 nM of HHT for 16 hours was determined by ATAC-Seq analysis. **B**. ATAC peak density at peak centers within 50 kb of a gene (enhancers) $\pm$ 5 kb were plotted with deepTools. **C**. Transcription Factor MOTIF analysis (HOMER) in decreased ATAC-Seq peaks in OCI-AML2 RUNX1$^{R174*/wt}$ cells treated with 100 nM of HHT. Transcription Factor motifs are rank sorted by -log10 p-value in HHT-treated versus control cells. **D-E**. IGV plot of sequence tag densities for H3K27Ac, BRD4 ChIP-Seq, P300 ChIP-Seq, and ATAC-Seq peaks at the RUNX1 and BCL2 locus in HHT-treated versus control OCI-AML2 RUNX1$^{R174*/wt}$ cells. Fold changes were calculated utilizing DiffReps. Log2 fold-changes in peak densities for H3K27Ac, BRD4, P300, and ATAC are denoted by blue (decreased) and red (increased) bars.

Figure S5. Treatment with HHT alters the transcriptome in mutant RUNX1 expressing AML cells. **A**. OCI-AML2 RUNX1$^{R174*/wt}$ cells were treated with 100 nM of HHT for 8 hours in biologic duplicates and RNA-Seq analysis was performed. The heatmap shows the number of mRNAs up or downregulated greater than 1.25-fold and with a p-value <0.05. **B-C**. GSEA plot and heatmap for OCI-AML2 and OCI-AML2 RUNX1$^{R174*/wt}$ cell mRNA expressions compared to REACTOME: Translation pathway and HALLMARK: Myc Targets V1. FDR q-values are < 0.1. **D**. Log2 fold-change in mRNA expression ($\geq$ 1.25-fold depleted) of REACTOME: Translation pathway genes in OCI-AML2 RUNX1$^{R174*/wt}$ treated with HHT versus control cells. **E**. Log2 fold-change in mRNA expression ($\geq$ 1.25-fold depleted) of HALLMARK: Myc Targets V1 genes in OCI-AML2 RUNX1$^{R174*/wt}$ treated with HHT versus control cells.

Figure S6. **Cotreatment with HHT and venetoclax or OTX015 exerts synergistic in vitro lethal activity against mtRUNX1 expressing AML cells**. **A.** OCI-AML2 RUNX1$^{R174*/wt}$ cells were treated with the indicated concentrations of HHT and/or venetoclax for 24 hours. Cells were stained with annexin V and To-Pro-3 iodide, and the % annexin V-positive, apoptotic cells were determined by flow cytometry. Bliss synergy scores were calculated utilizing SynergyFinder and graphed with GraphPad V8. **B**. OCI-AML5 cells were treated with the indicated concentrations of HHT and venetoclax for 48 hours. At the end of treatment, cells were stained with annexin V and To-Pro-3 iodide, and the % annexin V-positive, apoptotic cells were determined by flow cytometry. Bliss synergy scores were calculated utilizing SynergyFinder and graphed with GraphPad V8. **C**. Mono-Mac-1 cells were treated with the indicated concentrations of HHT and venetoclax for 48 hours. At the end of treatment, cells were stained with annexin V and To-Pro-3 iodide, and the % annexin V-positive, apoptotic cells were determined by flow cytometry. Bliss synergy scores were calculated utilizing SynergyFinder and graphed with GraphPad V8. OCI-AML2 RUNX1$^{R174*/wt}$ cells were treated with the indicated concentrations of HHT and/or venetoclax for 24 hours. Cells were stained with annexin V and To-Pro-3 iodide, and the % annexin V-positive, apoptotic cells were determined by flow cytometry. Bliss synergy scores were calculated utilizing SynergyFinder and graphed with GraphPad V8. **D**. OCI-AML2 cells were treated with the indicated concentrations of HHT and/or venetoclax for 48 hours. Cells were stained with annexin V and To-Pro-3 iodide, and the % annexin V-positive, apoptotic cells were determined by flow cytometry. Bliss synergy scores were calculated utilizing SynergyFinder and graphed with GraphPad V8. **E**. Normal CD34+ HPCs were treated with the indicated concentrations of HHT and venetoclax for 48 hours. The % non-viable cells were determined by To-Pro-3 iodide staining and flow cytometry. Values shown are a mean of four samples per combination. **F**. Densitometry analysis of protein expression changes due to treatment with HHT and/or venetoclax or OTX015 relative to the untreated control cells. * indicates protein expression alteration values that are significantly different ($p < 0.05$) in OCI-AML2 RUNX1 R174*/wt cells treated with HHT and/or venetoclax or OTX015 relative to the untreated control cells. **G**. Representative immunoblot analyses of OCI-AML5 cells treated with HHT and/or venetoclax for 18 hours. The expression of GAPDH served as the loading control. **H**. Representative immunoblot analyses of OCI-AML2 RUNX1$^{R174*/wt}$ cells treated with HHT and/or venetoclax or Etoposide for 18 hours. The expression of GAPDH served as the loading control. **I**. Oncoplot of next generation sequencing (NGS)-detected mutations in patient-derived de novo mtRUNX1 and wtRUNX1 expressing AML blasts utilized in these studies. **J**. OCI-AML2 RUNX1$^{R174*/wt}$ cells were treated with the indicated concentrations of HHT in the absence or presence of 250 nM of OTX015 for 48 hours. Cells were stained with annexin-V and To-Pro-3 iodide and the % apoptotic cells were determined by flow cytometry. Lines represent the mean of three independent experiments $\pm$ S.E.M. **K**. OCI-AML5 cells were treated with the indicated concentrations of HHT and/or OTX015 for 48 hours. At the end of treatment, cells were stained with annexin V and To-Pro-3 iodide, and the % annexin V-positive, apoptotic cells were determined by flow cytometry. Bliss synergy scores were calculated utilizing SynergyFinder and graphed with GraphPad V8. **L.** Mono-Mac-1 cells were treated with the indicated concentrations of HHT and/or OTX015 for 48 hours. At the end of treatment, cells were stained with annexin V and To-Pro-3 iodide, and the % annexin V-positive, apoptotic cells were determined by flow cytometry. Bliss synergy scores were calculated utilizing SynergyFinder and graphed with GraphPad V8. **M**. Densitometry analysis of protein expression changes due to treatment with HHT and/or OTX015 relative to the untreated control cells. * indicates protein expression alteration values that are significantly different ($p < 0.05$) in OCI-AML2 RUNX1$^{R174*/wt}$ cells treated with HHT and/or OTX015 relative to the untreated control cells. **N**. Representative immunoblot analysis of OCI-AML5 cells treated with the indicated concentrations of HHT and/or OTX015 for 16 hours. **O**. PD, wt RUNX1 expressing AML cells (n=8) were treated with the indicated

concentrations of HHT andor OTX015 for 48 hours. The % non-viable cells were determined by To-Pro-3 iodide staining and flow cytometry. Bliss synergy scores were calculated utilizing SynergyFinder and graphed with GraphPad V8. **P**. Normal CD34+ HPCs were treated with the indicated concentrations of HHT and/or OTX015 for 48 hours. The % non-viable cells were determined by To-Pro-3 iodide staining and flow cytometry.

Table S1. The RUNX1 mutation(s) identified by NextGen sequencing in the 14 patient-derived mtRUNX1 expressing AML samples utilized in these studies. The nucleotide alteration in the DNA and the resulting protein alteration are shown for each sample.

Figure S7. Cotreatment with OM and venetoclax or OTX015 reduces in vivo leukemia burden and significantly improves survival of mice bearing mtRUNX1 AML xenografts. **A**. Bioluminescent flux in NSG mice bearing OCI-AML2 RUNX1$^{R174*/wt}$ GFP/Luc xenografts treated for two weeks with omacetaxine mepesuccinate (OM) (1 mg/kg s. c., daily x 5 days per week), venetoclax (Ven) (20 mg/kg, P.O., daily x 5 days per week) or combination of omacetaxine with venetoclax. Representative bioluminescent images of mice in each cohort treated for two weeks, as indicated. **B**. Median survival (Days) of mice bearing PDX mtRUNX1 AML#8-GFP/Luc xenografts treated for six weeks as indicated. **C**. Statistical comparison of overall survival (OS) curves from PDX mtRUNX1 AML#8-GFP/Luc xenograft bearing mice treated with OM and/or Ven or OTX015.

Fig. S1

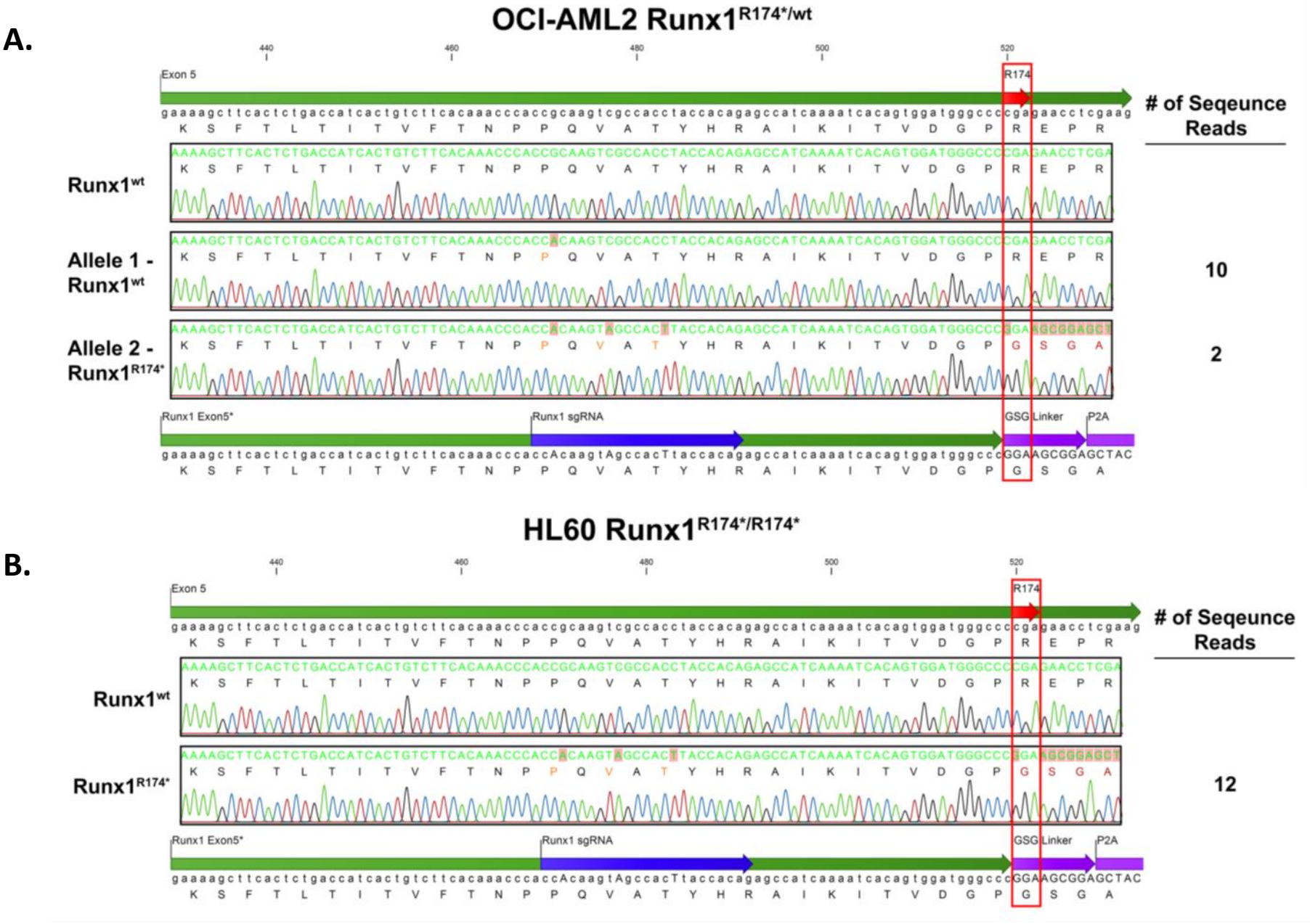
A.
OCI-AML2 Runx1R174*/wt
Exon 5
R174
# of Seqeunce Reads
Runx1wt
Allele 1 - Runx1wt
10
Allele 2 - Runx1R174*
2
Runx1 Exon5*
Runx1 sgRNA
GSG Linker
P2A
B.
HL60 Runx1R174*/R174*
Exon 5
R174
# of Seqeunce Reads
Runx1wt
Runx1R174*
12
Runx1 Exon5*
Runx1 sgRNA
GSG Linker
P2A

Fig. S1

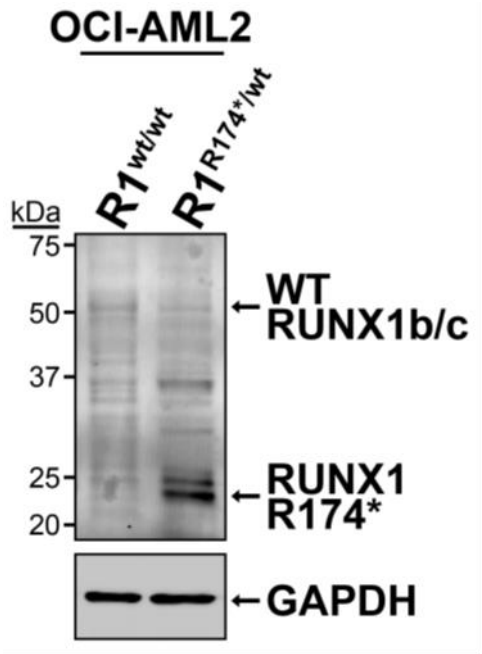
C.
OCI-AML2
R1wt/wt
R1R174*/wt
kDa
75
50
37
25
20
WT
RUNX1b/c
RUNX1
R174*
GAPDH

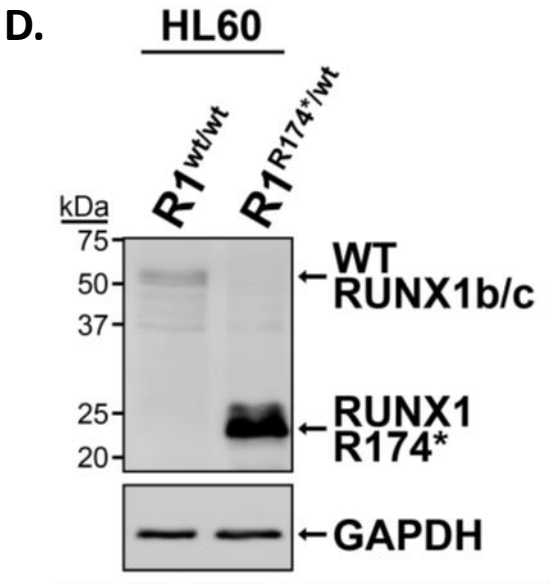
D.
HL60
R1wt/wt
R1R174*/wt
kDa
75
50
37
25
20
WT
RUNX1b/c
RUNX1
R174*
GAPDH

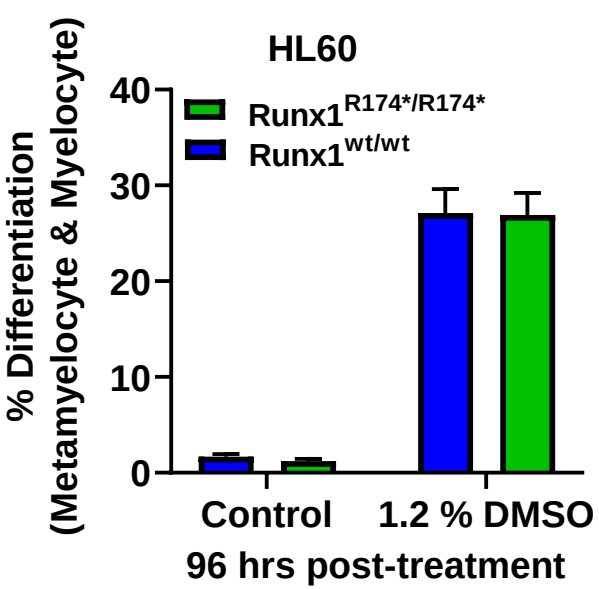
F.
HL60
Runx1R174*/R174*
Runx1wt/wt
% Differentiation
(Metamyelocyte & Myelocyte)
40
30
20
10
0
Control
1.2 % DMSO
96 hrs post-treatment

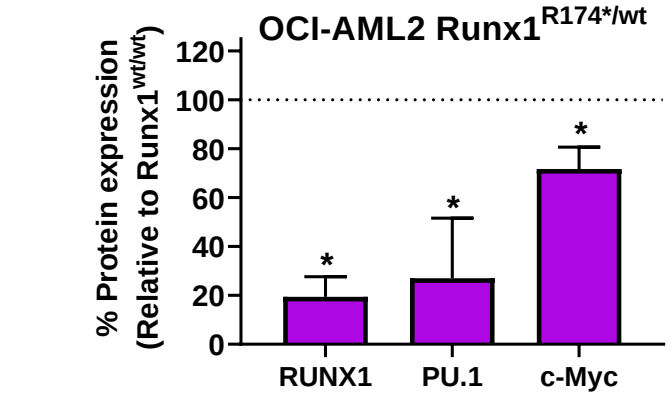
E.
OCI-AML2 Runx1R174*/wt
% Protein expression
(Relative to Runx1wt/wt)
120
100
80
60
40
20
0
*
*
*
RUNX1
PU.1
c-Myc

Fig. S2

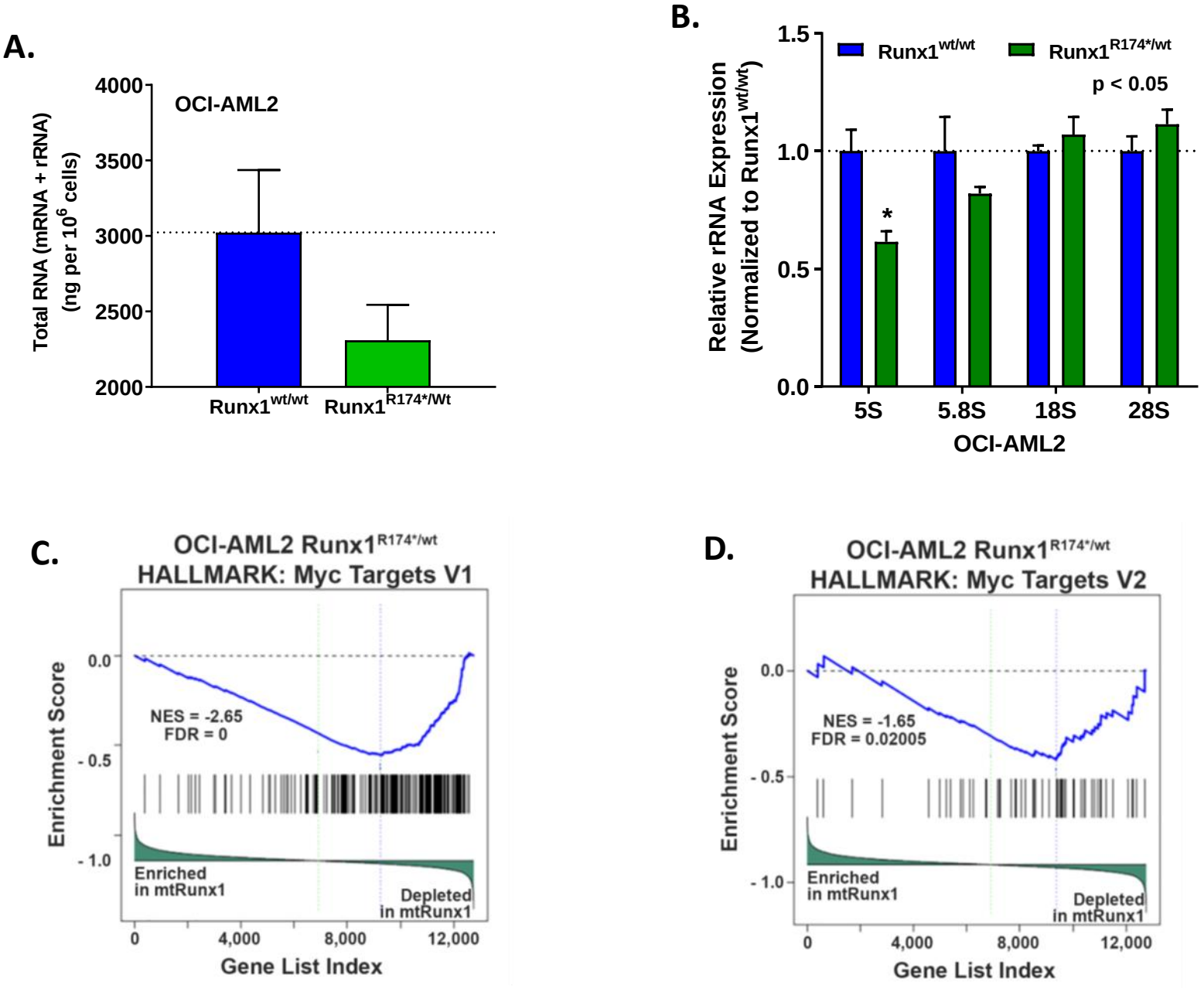
A.
OCI-AML2
Total RNA (mRNA + rRNA)
(ng per 10^6 cells)
4000
3500
3000
2500
2000
Runx1wt/wt
Runx1R174*/Wt
B.
Runx1wt/wt
Runx1R174*/wt
p < 0.05
Relative rRNA Expression
(Normalized to Runx1wt/wt)
1.5
1.0
0.5
0.0
*
5S
5.8S
18S
28S
OCI-AML2
C.
OCI-AML2 Runx1R174*/wt
HALLMARK: Myc Targets V1
Enrichment Score
0.0
- 0.5
- 1.0
NES = -2.65
FDR = 0
Enriched
in mtRunx1
Depleted
in mtRunx1
0
4,000
8,000
12,000
Gene List Index
D.
OCI-AML2 Runx1R174*/wt
HALLMARK: Myc Targets V2
Enrichment Score
0.0
- 0.5
- 1.0
NES = -1.65
FDR = 0.02005
Enriched
in mtRunx1
Depleted
in mtRunx1
0
4,000
8,000
12,000
Gene List Index

E.

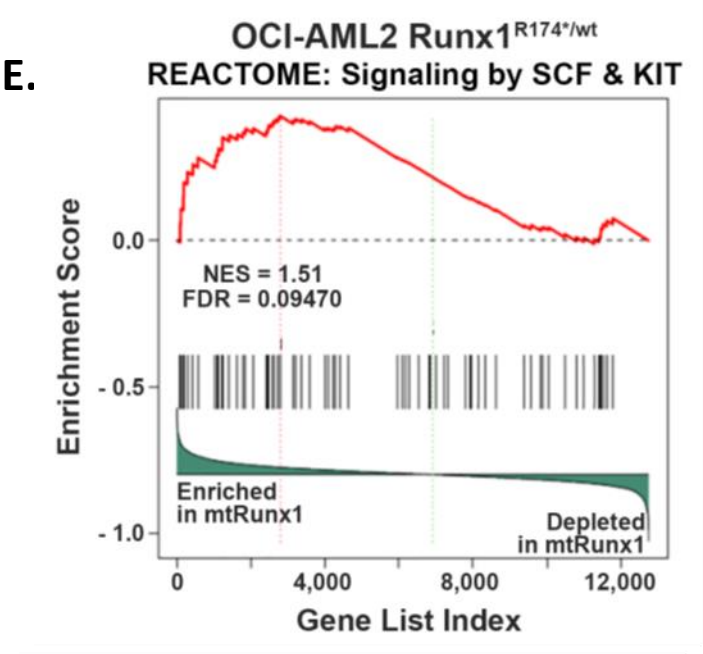

F.

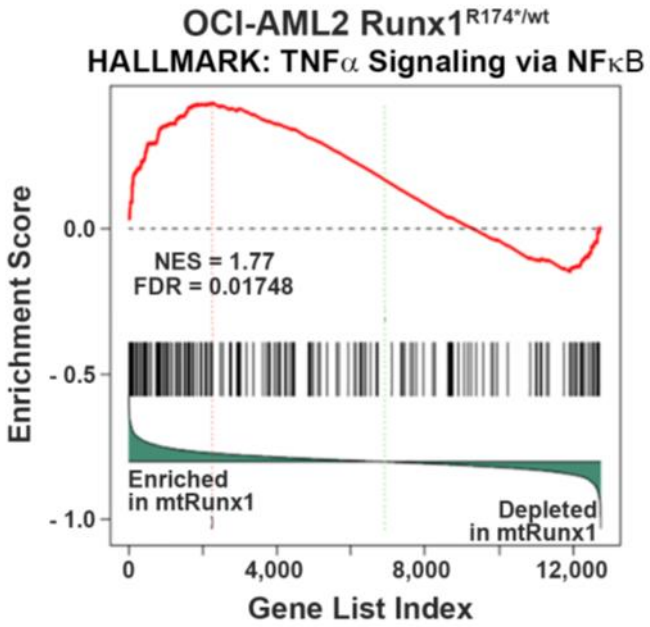

G.

Fractions	% AUC in mtRunx1 (Relative to wtRunx1)
40S	76%
60S	67%
80S	95%
Polysome	93%

Fig. S2

Fig. S2

H.

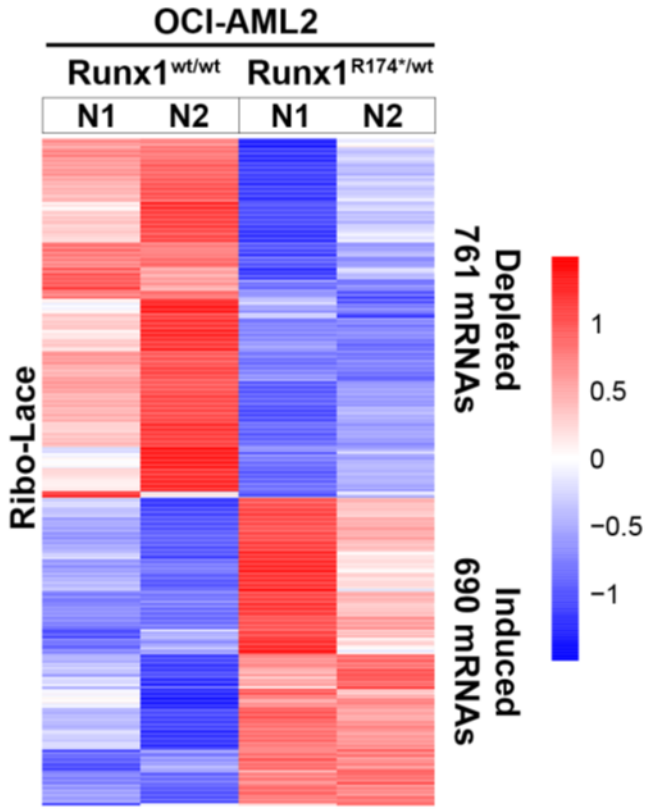
OCI-AML2
Runx1wt/wt
Runx1R174*/wt
N1
N2
N1
N2
Ribo-Lace
Depleted
761 mRNAs
Induced
690 mRNAs
1
0.5
0
−0.5
−1

I.

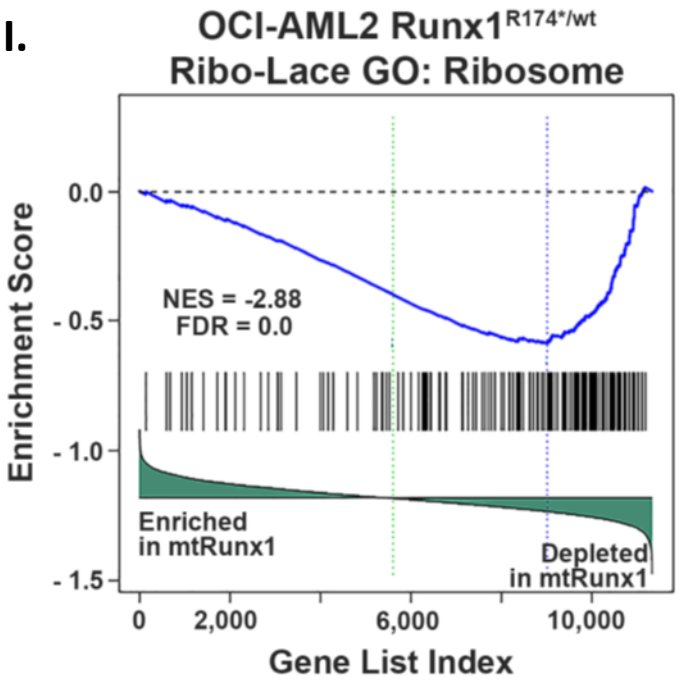
OCI-AML2 Runx1R174*/wt
Ribo-Lace GO: Ribosome
Enrichment Score
0.0
- 0.5
- 1.0
- 1.5
NES = -2.88
FDR = 0.0
Enriched
in mtRunx1
Depleted
in mtRunx1
0
2,000
6,000
10,000
Gene List Index

Fig. S3

A.

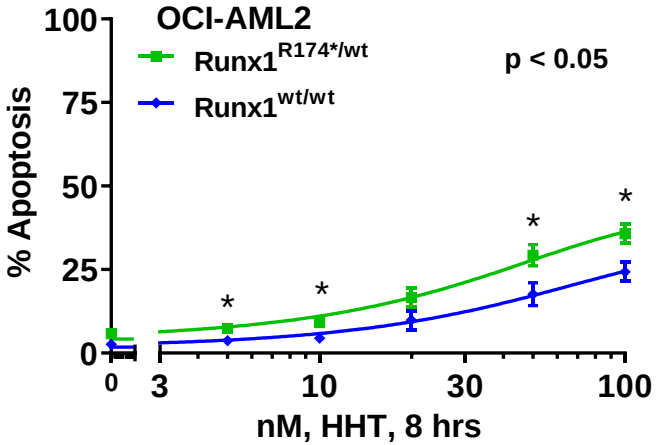
OCI-AML2
Runx1R174*/wt
Runx1wt/wt
p < 0.05
% Apoptosis
100
75
50
25
0
0
3
10
30
100
nM, HHT, 8 hrs

B.

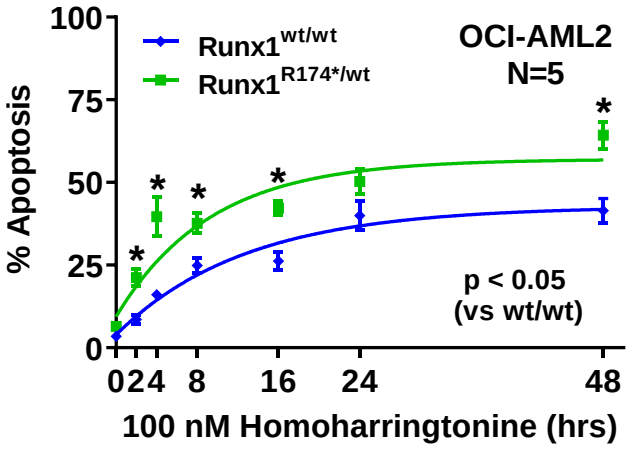
Runx1wt/wt
Runx1R174*/wt
OCI-AML2
N=5
p < 0.05
(vs wt/wt)
% Apoptosis
100
75
50
25
0
0 2 4 8 16 24 48
100 nM Homoharringtonine (hrs)

C.

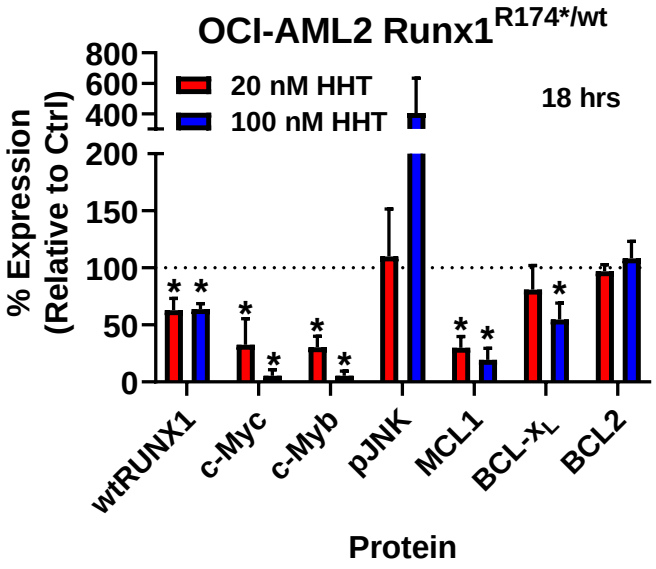
OCI-AML2 Runx1R174*/wt
20 nM HHT
100 nM HHT
18 hrs
% Expression
(Relative to Ctrl)
800
600
400
200
150
100
50
0
wtRUNX1
c-Myc
c-Myb
pJNK
MCL1
BCL-xL
BCL2
Protein

D.

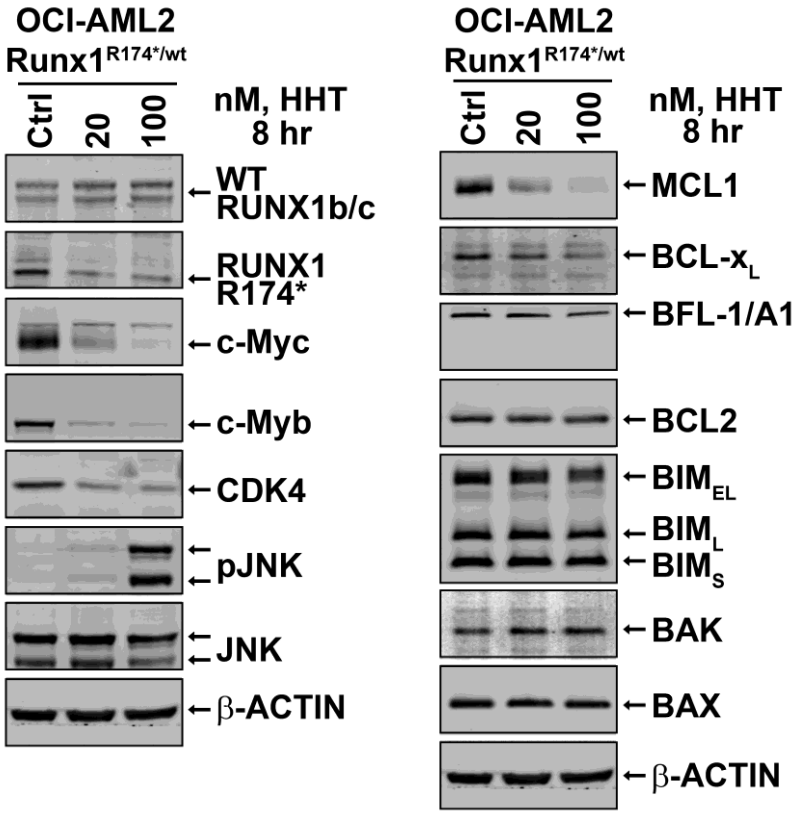
OCI-AML2
Runx1R174*/wt
Ctrl
20
100
nM, HHT
8 hr
WT
RUNX1b/c
RUNX1
R174*
c-Myc
c-Myb
CDK4
pJNK
JNK
β-ACTIN
OCI-AML2
Runx1R174*/wt
Ctrl
20
100
nM, HHT
8 hr
MCL1
BCL-xL
BFL-1/A1
BCL2
BIMEL
BIML
BIMS
BAK
BAX
β-ACTIN

E.

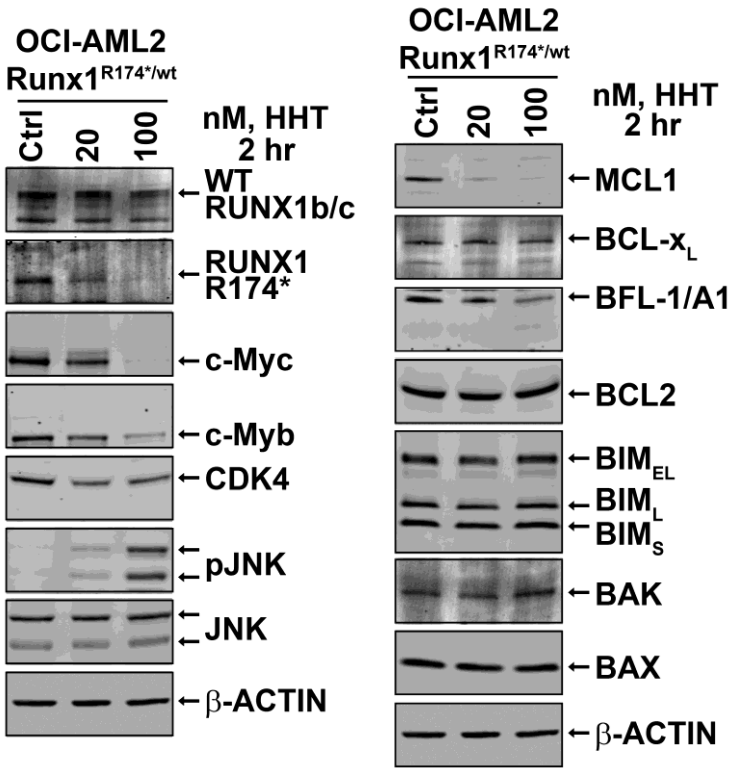

F.

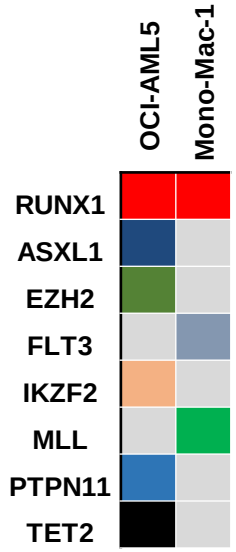

Cell line	Mutation in RUNX1 DNA	Protein Change
OCI-AML5	c.370-371 insTGCTA	p.T124fs*6
Mono-Mac-1	c. 321G>A	p.A107V

G.

	Mean % Non-Viable (20 nM HHT)	Significance (Relative to mtRunx1)	Mean % Non-Viable (50 nM HHT)	Significance (Relative to mtRunx1)
mtRunx1 AML (N=9)	40.70 ± 4.94	N/A	47.15 ± 5.06	N/A
wtRunx1 AML (N=14)	27.90 ± 3.23	0.024	32.72 ± 3.10	0.021
Normal CD34+ HPC (N=4)	20.60 ± 1.47	0.028	24.05 ± 1.77	0.010

H.

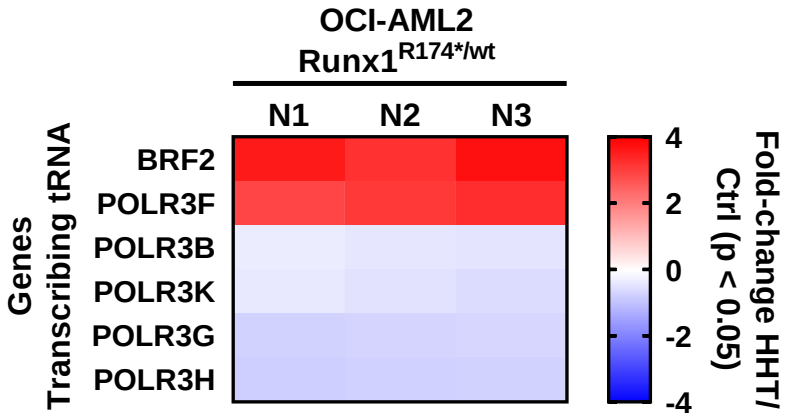
OCI-AML2
Runx1R174*/wt
N1
N2
N3
BRF2
POLR3F
POLR3B
POLR3K
POLR3G
POLR3H
Genes
Transcribing tRNA
4
2
0
-2
-4
Fold-change HHT/
Ctrl (p < 0.05)

I.

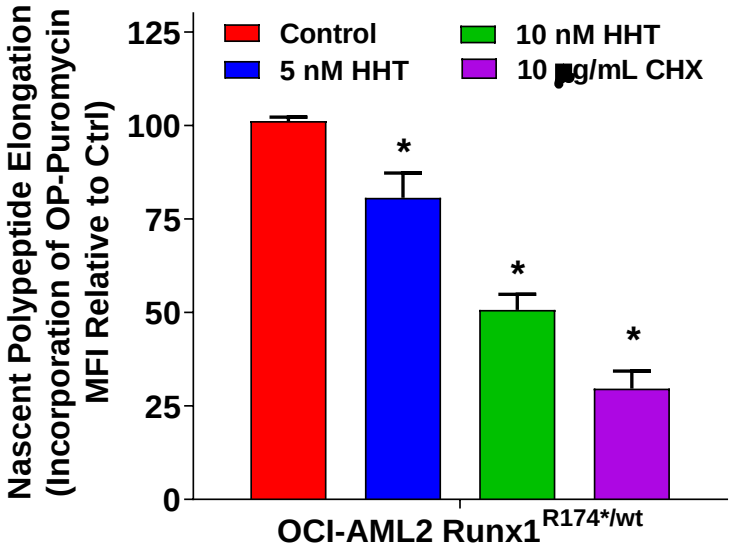
Nascent Polypeptide Elongation
(Incorporation of OP-Puromycin
MFI Relative to Ctrl)
125
100
75
50
25
0
Control
5 nM HHT
10 nM HHT
10 µg/mL CHX
*
*
*
OCI-AML2 Runx1R174*/wt

J.

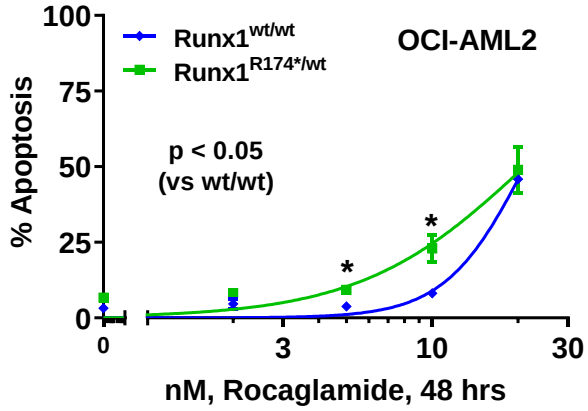
100
75
50
25
0
% Apoptosis
Runx1wt/wt
Runx1R174*/wt
OCI-AML2
p < 0.05
(vs wt/wt)
*
*
0
3
10
30
nM, Rocaglamide, 48 hrs

K.

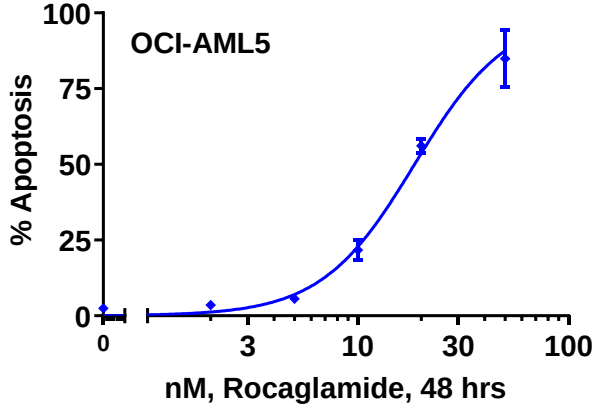
100
75
50
25
0
% Apoptosis
OCI-AML5
0
3
10
30
100
nM, Rocaglamide, 48 hrs

L.

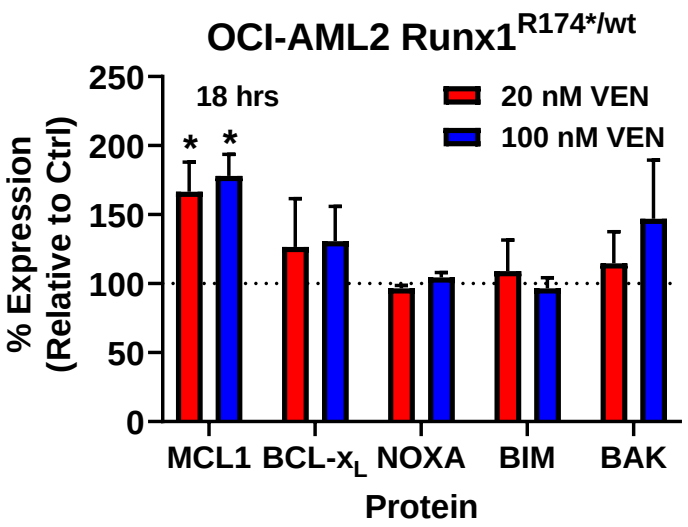
OCI-AML2 Runx1R174*/wt
18 hrs
20 nM VEN
100 nM VEN
% Expression (Relative to Ctrl)
250
200
150
100
50
0
*
*
MCL1
BCL-xL
NOXA
BIM
BAK
Protein

M.

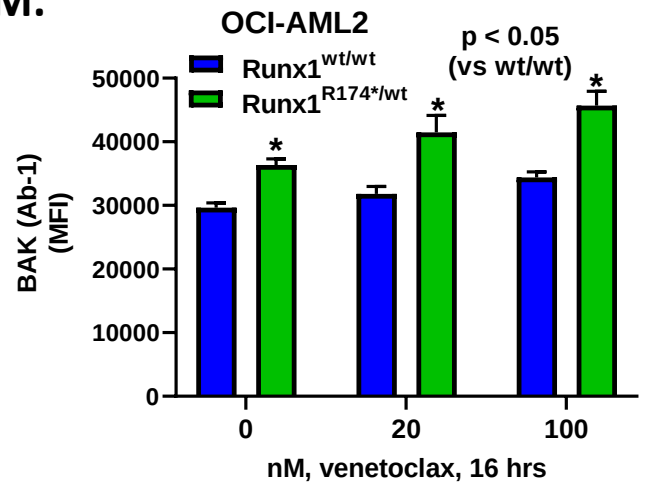
OCI-AML2
p < 0.05
(vs wt/wt)
Runx1wt/wt
Runx1R174*/wt
BAK (Ab-1) (MFI)
50000
40000
30000
20000
10000
0
*
*
*
0
20
100
nM, venetoclax, 16 hrs

Fig. S4

A.

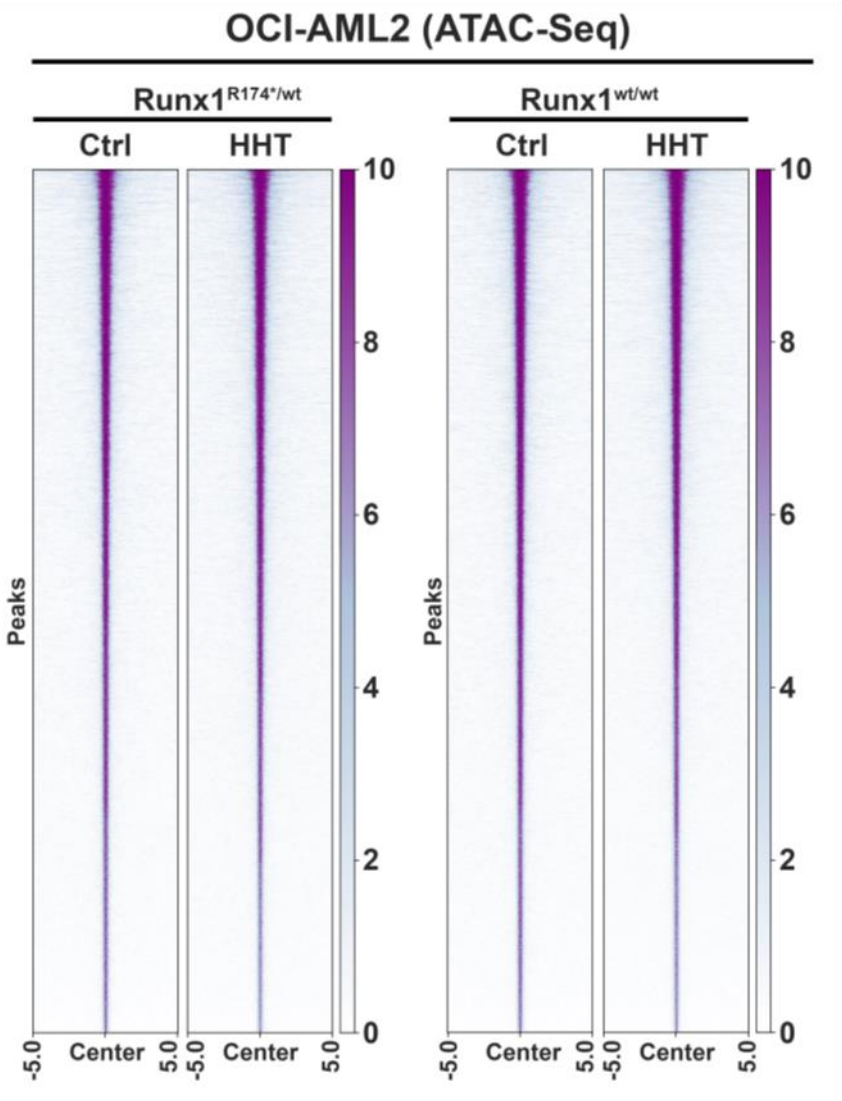
OCI-AML2 (ATAC-Seq)
Runx1R174*/wt
Runx1wt/wt
Ctrl
HHT
Ctrl
HHT
Peaks
Peaks
10
8
6
4
2
0
-5.0
Center
5.0
-5.0
Center
5.0
-5.0
Center
5.0
-5.0
Center
5.0

B.

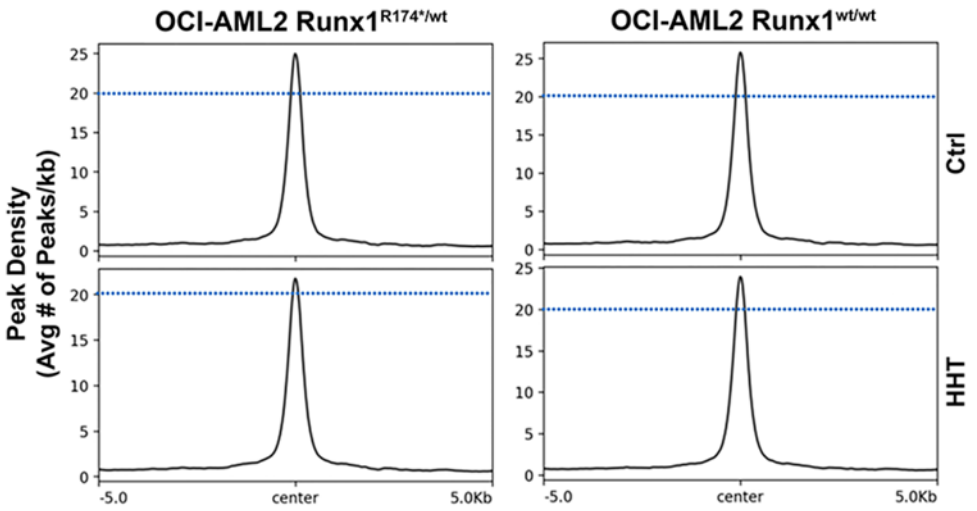
OCI-AML2 Runx1R174*/wt
OCI-AML2 Runx1wt/wt
Peak Density
(Avg # of Peaks/kb)
25
20
15
10
5
0
Ctrl
HHT
-5.0
center
5.0Kb
-5.0
center
5.0Kb

C.

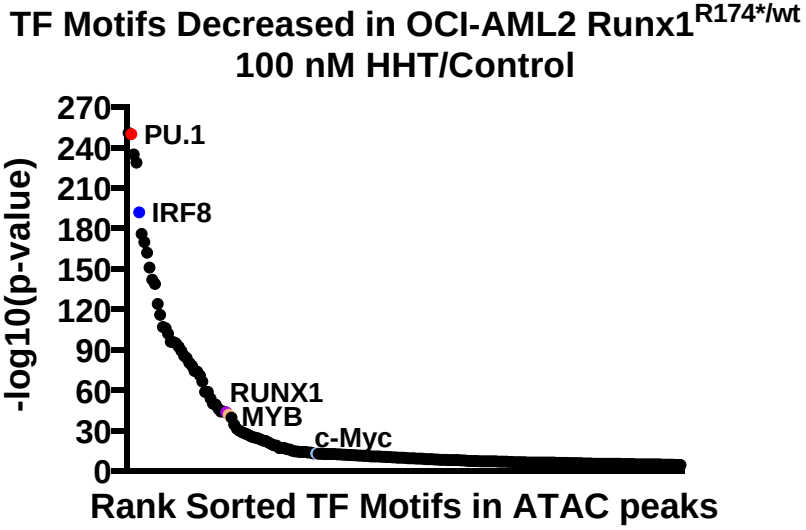
TF Motifs Decreased in OCI-AML2 Runx1R174*/wt
100 nM HHT/Control
-log10(p-value)
270
240
210
180
150
120
90
60
30
0
PU.1
IRF8
RUNX1
MYB
c-Myc
Rank Sorted TF Motifs in ATAC peaks

Fig. S4

D.

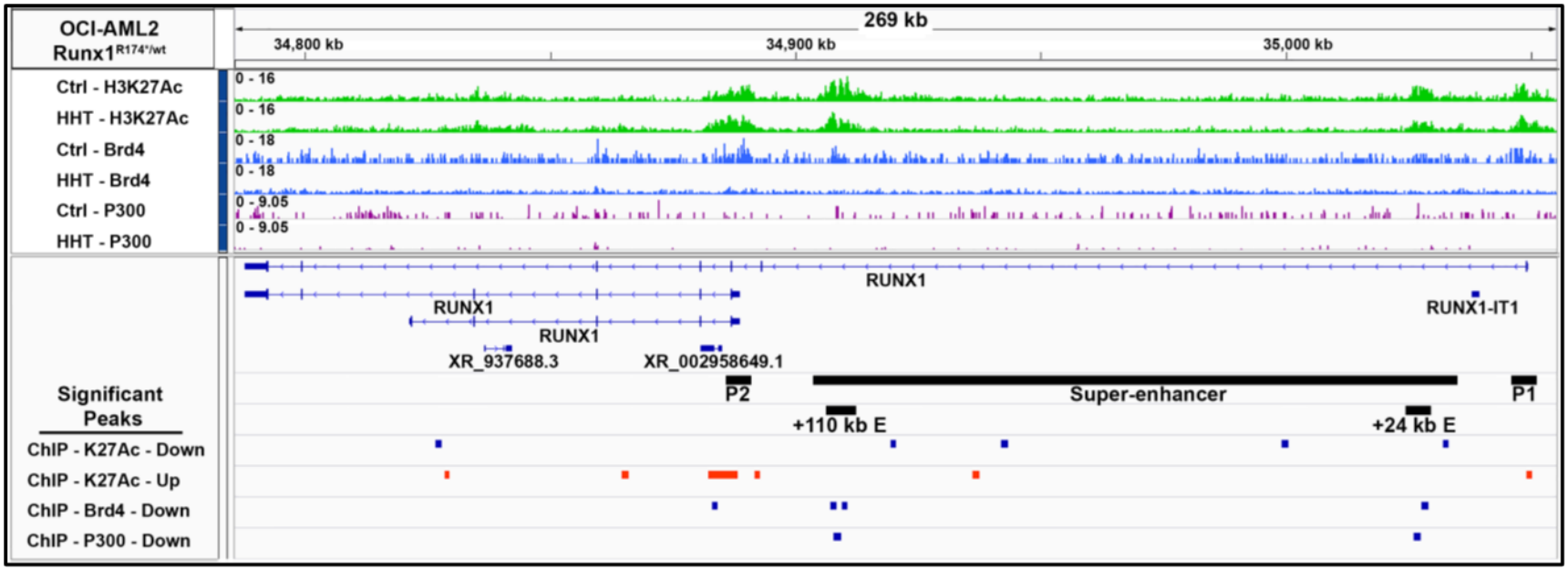
OCI-AML2
Runx1R174*/wt
269 kb
34,800 kb
34,900 kb
35,000 kb
Ctrl - H3K27Ac
HHT - H3K27Ac
Ctrl - Brd4
HHT - Brd4
Ctrl - P300
HHT - P300
0 - 16
0 - 16
0 - 18
0 - 18
0 - 9.05
0 - 9.05
RUNX1
RUNX1
RUNX1
RUNX1-IT1
XR_937688.3
XR_002958649.1
P2
Super-enhancer
P1
+110 kb E
+24 kb E
Significant Peaks
ChIP - K27Ac - Down
ChIP - K27Ac - Up
ChIP - Brd4 - Down
ChIP - P300 - Down

E.

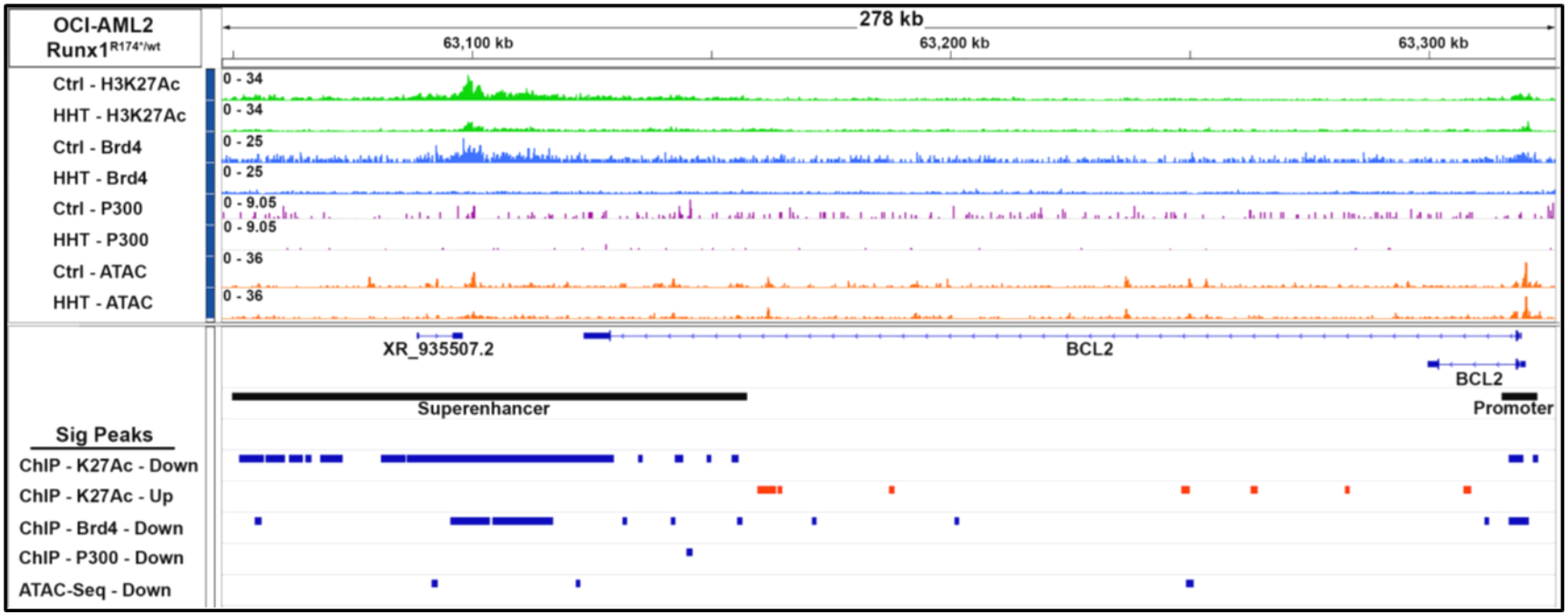
OCI-AML2
Runx1R174*/wt
278 kb
63,100 kb
63,200 kb
63,300 kb
Ctrl - H3K27Ac
HHT - H3K27Ac
Ctrl - Brd4
HHT - Brd4
Ctrl - P300
HHT - P300
Ctrl - ATAC
HHT - ATAC
0 - 34
0 - 34
0 - 25
0 - 25
0 - 9.05
0 - 9.05
0 - 36
0 - 36
XR_935507.2
BCL2
BCL2
Superenhancer
Promoter
Sig Peaks
ChIP - K27Ac - Down
ChIP - K27Ac - Up
ChIP - Brd4 - Down
ChIP - P300 - Down
ATAC-Seq - Down

Fig. S5

A.

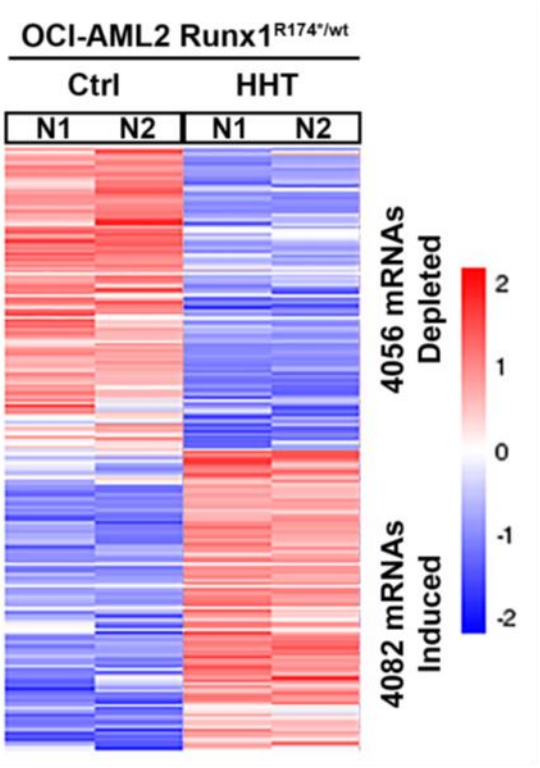
OCI-AML2 Runx1R174*/wt
Ctrl
HHT
N1
N2
N1
N2
4056 mRNAs Depleted
4082 mRNAs Induced
2
1
0
-1
-2

B.

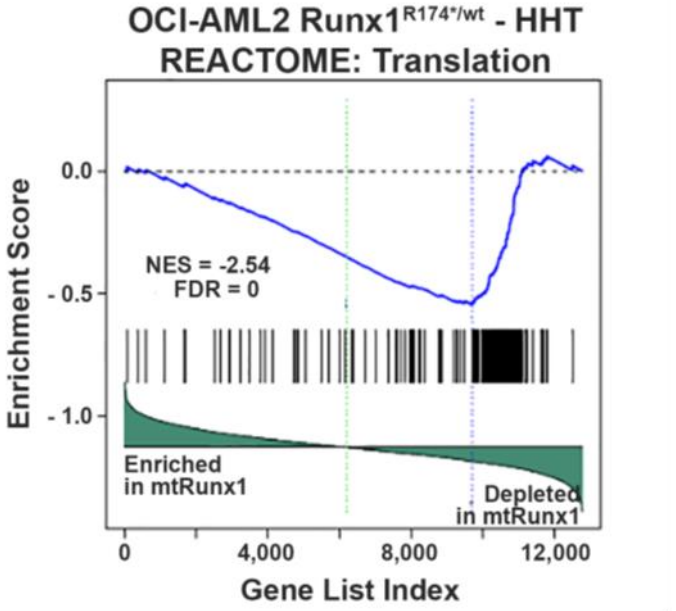
OCI-AML2 Runx1R174*/wt - HHT
REACTOME: Translation
Enrichment Score
0.0
- 0.5
- 1.0
NES = -2.54
FDR = 0
Enriched in mtRunx1
Depleted in mtRunx1
0
4,000
8,000
12,000
Gene List Index

C.

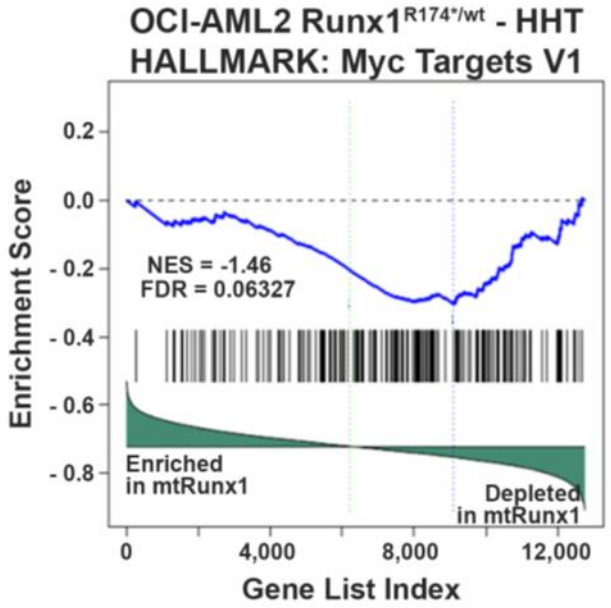
OCI-AML2 Runx1R174*/wt - HHT
HALLMARK: Myc Targets V1
Enrichment Score
0.2
0.0
- 0.2
- 0.4
- 0.6
- 0.8
NES = -1.46
FDR = 0.06327
Enriched in mtRunx1
Depleted in mtRunx1
0
4,000
8,000
12,000
Gene List Index

Fig. S5

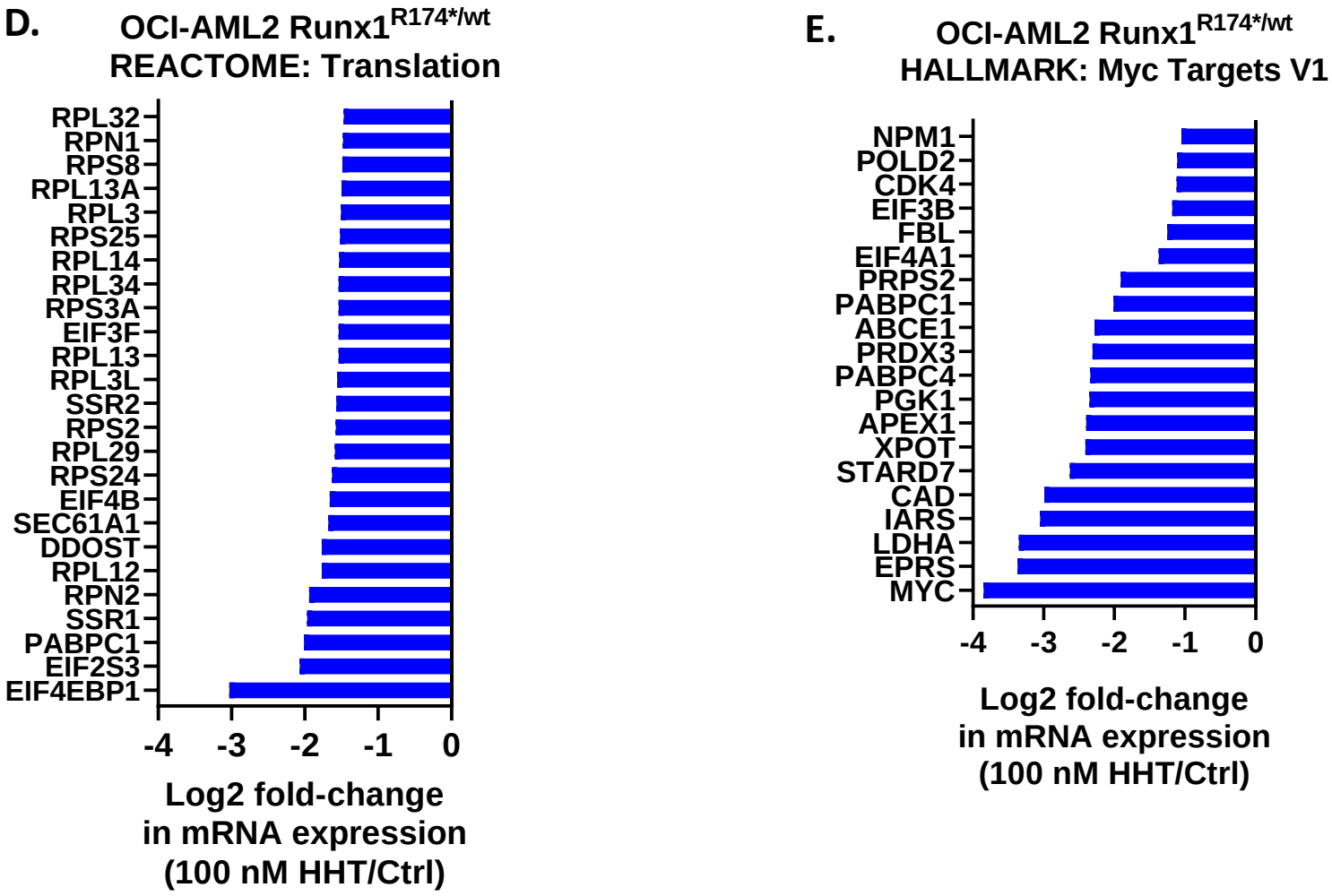
D.
OCI-AML2 Runx1R174*/wt
REACTOME: Translation
RPL32
RPN1
RPS8
RPL13A
RPL3
RPS25
RPL14
RPL34
RPS3A
EIF3F
RPL13
RPL3L
SSR2
RPS2
RPL29
RPS24
EIF4B
SEC61A1
DDOST
RPL12
RPN2
SSR1
PABPC1
EIF2S3
EIF4EBP1
-4
-3
-2
-1
0
Log2 fold-change
in mRNA expression
(100 nM HHT/Ctrl)
E.
OCI-AML2 Runx1R174*/wt
HALLMARK: Myc Targets V1
NPM1
POLD2
CDK4
EIF3B
FBL
EIF4A1
PRPS2
PABPC1
ABCE1
PRDX3
PABPC4
PGK1
APEX1
XPOT
STARD7
CAD
IARS
LDHA
EPRS
MYC
-4
-3
-2
-1
0
Log2 fold-change
in mRNA expression
(100 nM HHT/Ctrl)

Fig. S6

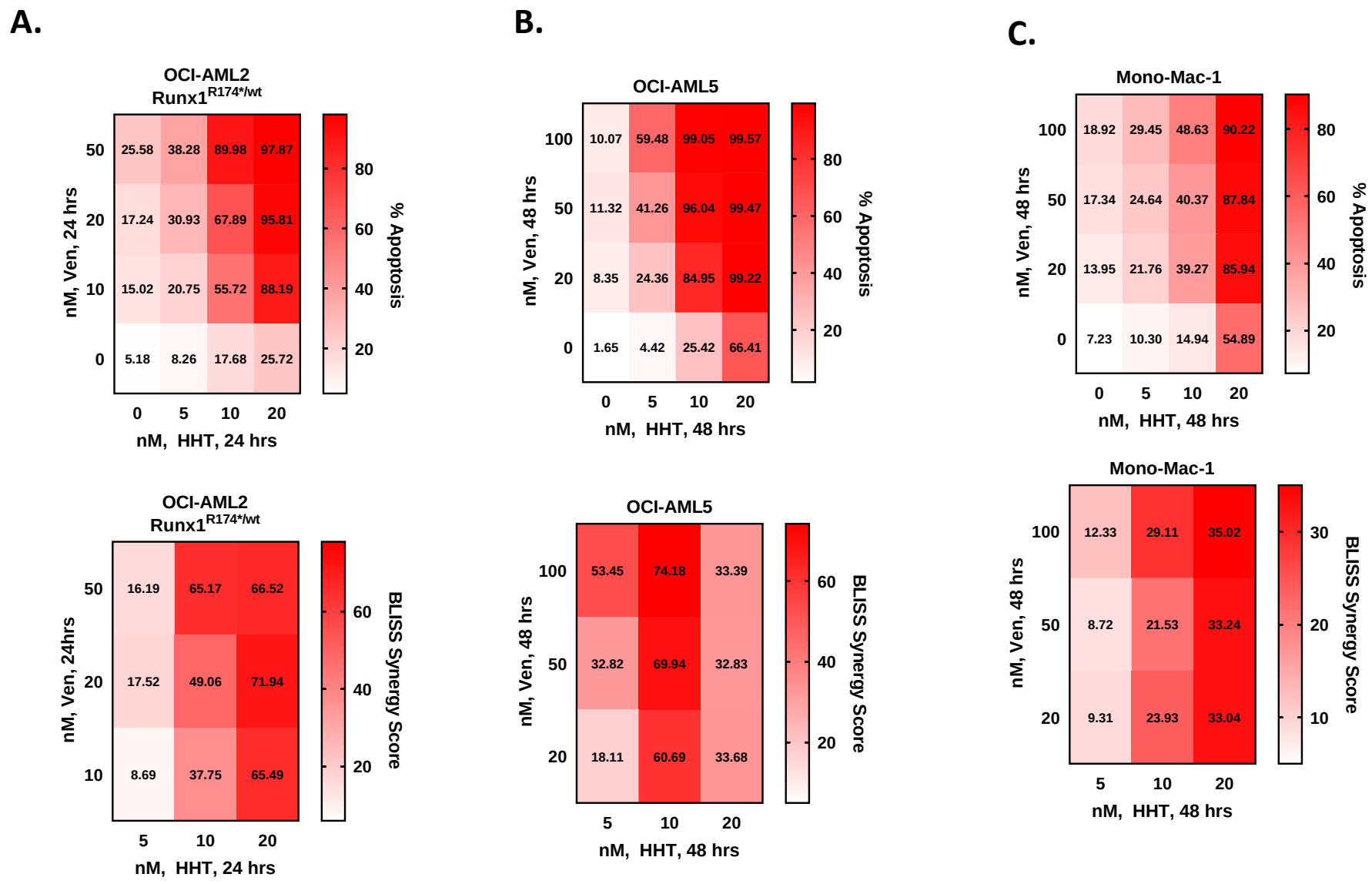
A.
OCI-AML2
Runx1R174*/wt
nM, Ven, 24 hrs
50
20
10
0
25.58
38.28
89.98
97.87
17.24
30.93
67.89
95.81
15.02
20.75
55.72
88.19
5.18
8.26
17.68
25.72
0
5
10
20
nM, HHT, 24 hrs
80
60
40
20
% Apoptosis
OCI-AML2
Runx1R174*/wt
nM, Ven, 24hrs
50
20
10
16.19
65.17
66.52
17.52
49.06
71.94
8.69
37.75
65.49
5
10
20
nM, HHT, 24 hrs
60
40
20
BLISS Synergy Score
B.
OCI-AML5
nM, Ven, 48 hrs
100
50
20
0
10.07
59.48
99.05
99.57
11.32
41.26
96.04
99.47
8.35
24.36
84.95
99.22
1.65
4.42
25.42
66.41
0
5
10
20
nM, HHT, 48 hrs
80
60
40
20
% Apoptosis
OCI-AML5
nM, Ven, 48 hrs
100
50
20
53.45
74.18
33.39
32.82
69.94
32.83
18.11
60.69
33.68
5
10
20
nM, HHT, 48 hrs
60
40
20
BLISS Synergy Score
C.
Mono-Mac-1
nM, Ven, 48 hrs
100
50
20
0
18.92
29.45
48.63
90.22
17.34
24.64
40.37
87.84
13.95
21.76
39.27
85.94
7.23
10.30
14.94
54.89
0
5
10
20
nM, HHT, 48 hrs
80
60
40
20
% Apoptosis
Mono-Mac-1
nM, Ven, 48 hrs
100
50
20
12.33
29.11
35.02
8.72
21.53
33.24
9.31
23.93
33.04
5
10
20
nM, HHT, 48 hrs
30
20
10
BLISS Synergy Score

Fig. S6

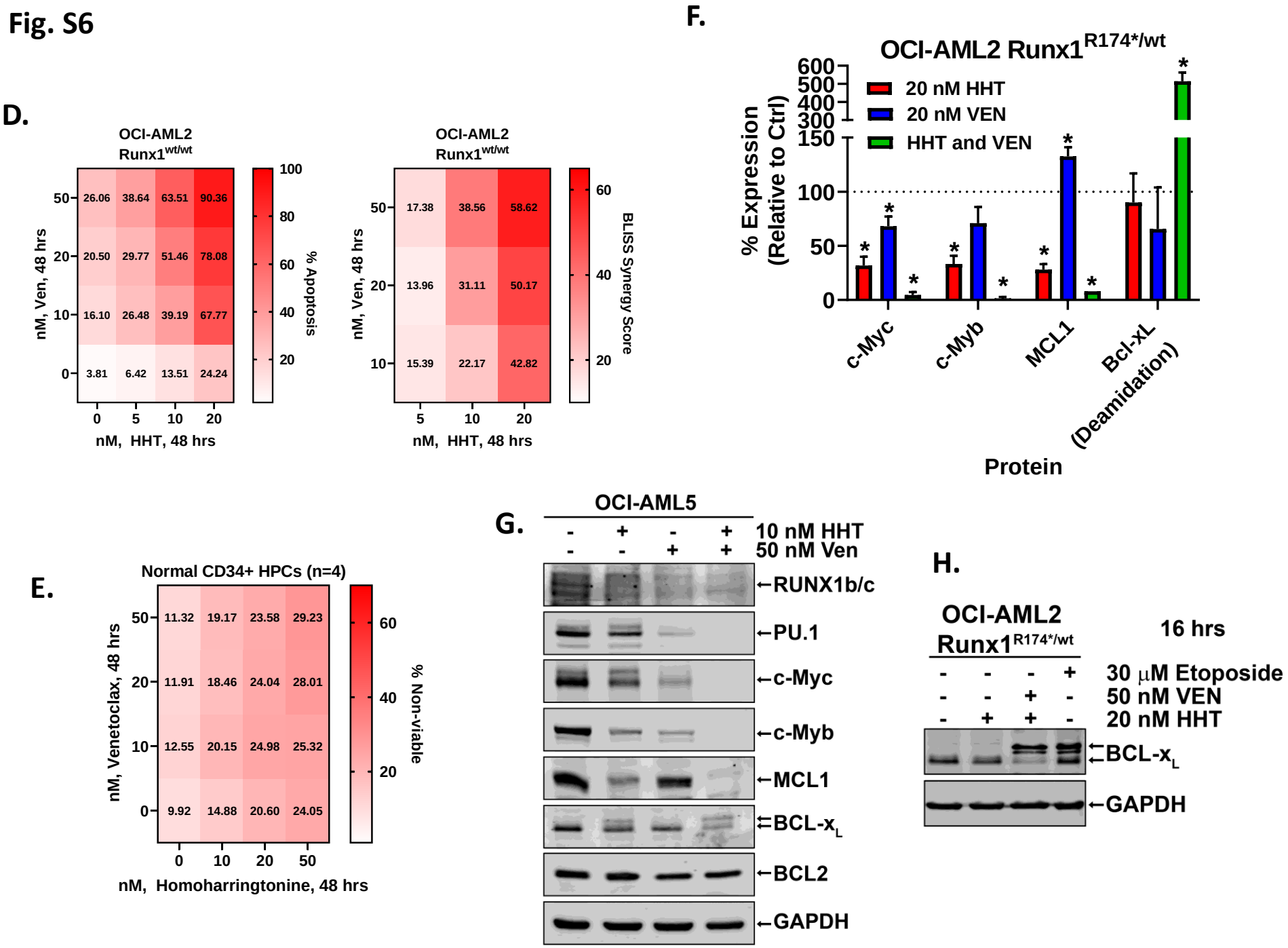
D.
OCI-AML2
Runx1wt/wt
nM, Ven, 48 hrs
nM, HHT, 48 hrs
% Apoptosis
BLISS Synergy Score
E.
Normal CD34+ HPCs (n=4)
nM, Venetoclax, 48 hrs
nM, Homoharringtonine, 48 hrs
% Non-viable
F.
OCI-AML2 Runx1R174*/wt
20 nM HHT
20 nM VEN
HHT and VEN
% Expression (Relative to Ctrl)
c-Myc
c-Myb
MCL1
Bcl-xL (Deamidation)
Protein
G.
OCI-AML5
10 nM HHT
50 nM Ven
RUNX1b/c
PU.1
c-Myc
c-Myb
MCL1
BCL-xL
BCL2
GAPDH
H.
OCI-AML2
Runx1R174*/wt
16 hrs
30 μM Etoposide
50 nM VEN
20 nM HHT
BCL-xL
GAPDH

Fig. S6

I.

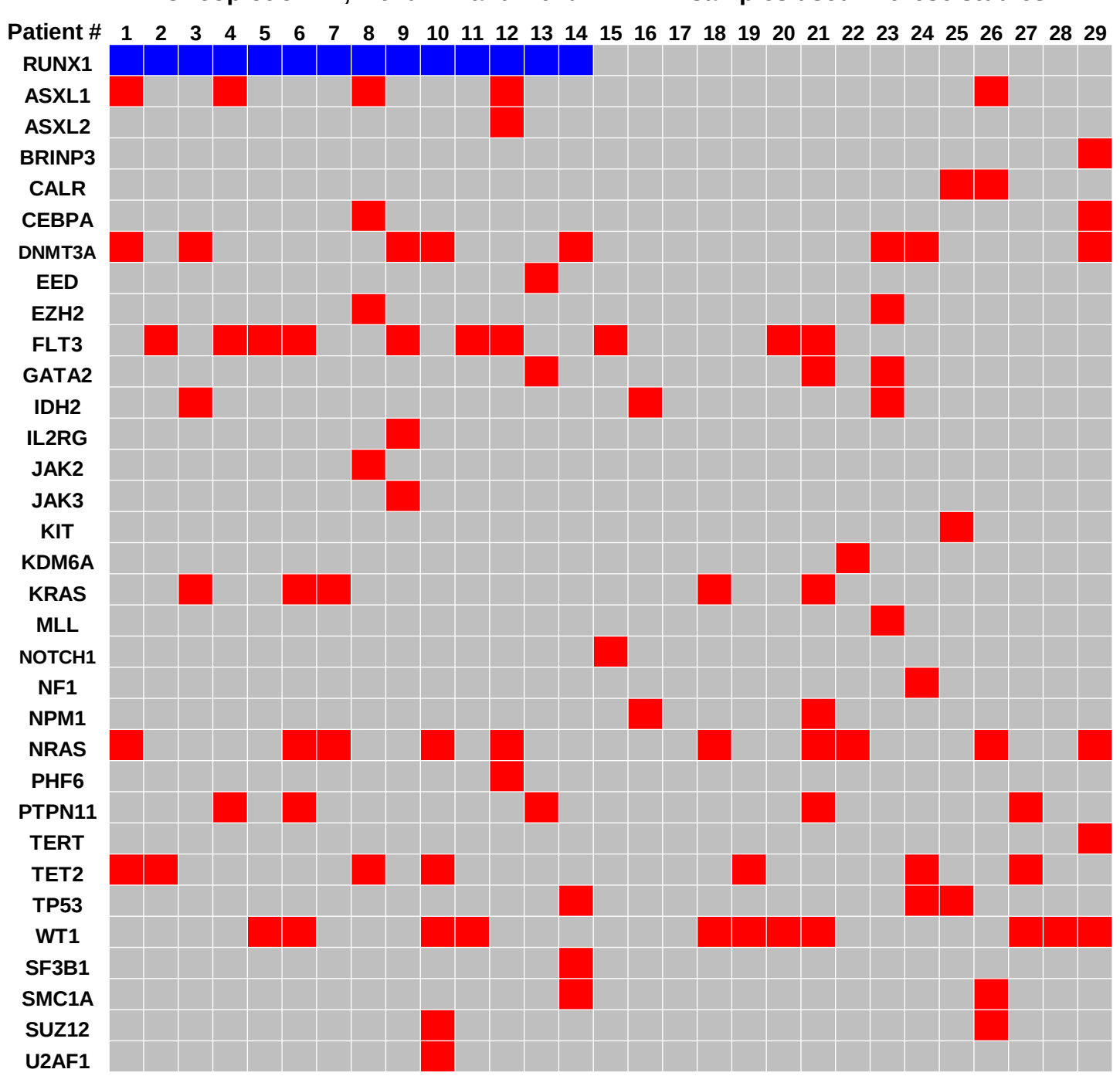
Oncoplot of PD, mtRunx1 and wtRunx1 AML samples used in these studies
Patient #
1 2 3 4 5 6 7 8 9 10 11 12 13 14 15 16 17 18 19 20 21 22 23 24 25 26 27 28 29
RUNX1
ASXL1
ASXL2
BRINP3
CALR
CEBPA
DNMT3A
EED
EZH2
FLT3
GATA2
IDH2
IL2RG
JAK2
JAK3
KIT
KDM6A
KRAS
MLL
NOTCH1
NF1
NPM1
NRAS
PHF6
PTPN11
TERT
TET2
TP53
WT1
SF3B1
SMC1A
SUZ12
U2AF1

Fig. S6

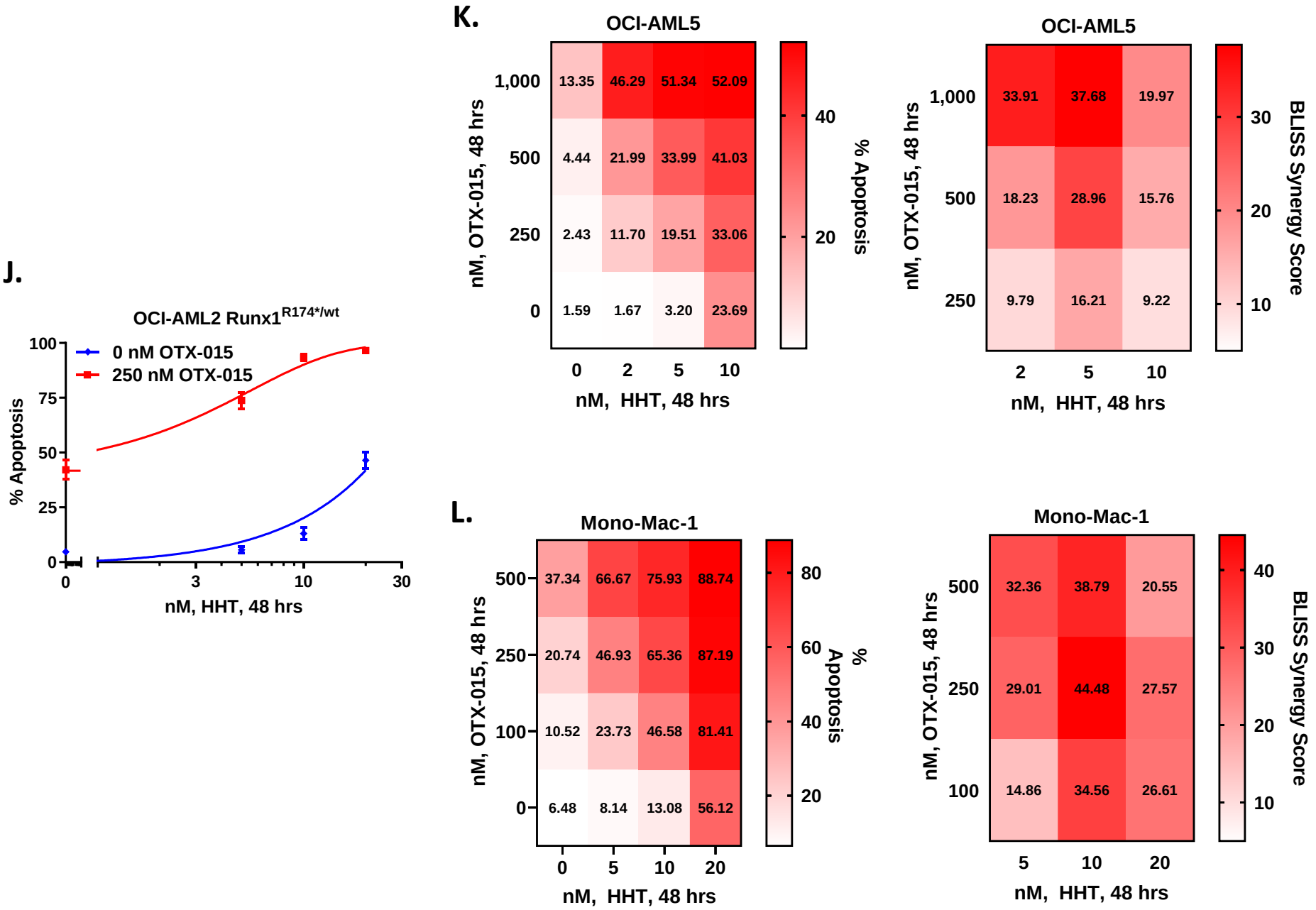
J.
OCI-AML2 Runx1R174*/wt
0 nM OTX-015
250 nM OTX-015
% Apoptosis
nM, HHT, 48 hrs
K.
OCI-AML5
nM, OTX-015, 48 hrs
nM, HHT, 48 hrs
% Apoptosis
BLISS Synergy Score
L.
Mono-Mac-1

Fig. S6

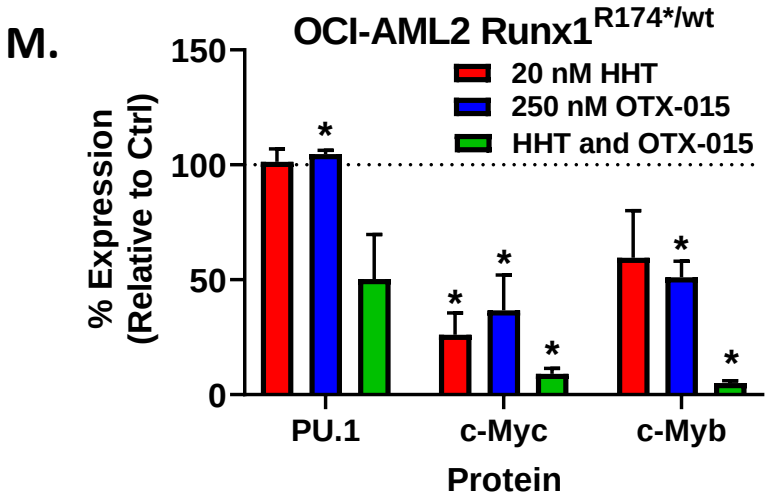
M.
OCI-AML2 Runx1R174*/wt
20 nM HHT
250 nM OTX-015
HHT and OTX-015
% Expression (Relative to Ctrl)
150
100
50
0
PU.1
c-Myc
c-Myb
Protein

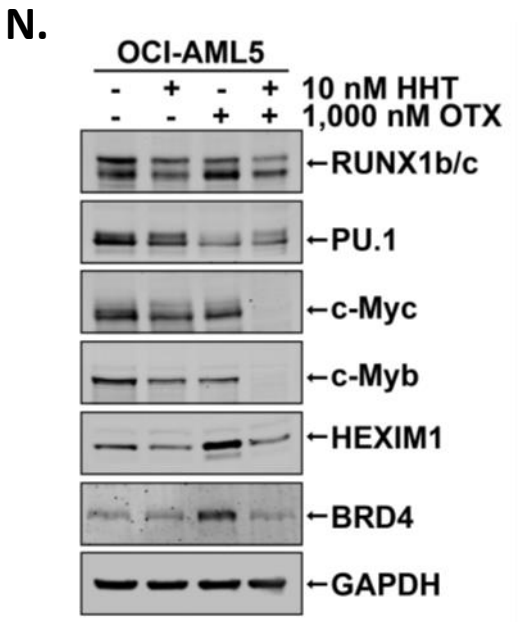
N.
OCI-AML5
- + - + 10 nM HHT
- - + + 1,000 nM OTX
←RUNX1b/c
←PU.1
←c-Myc
←c-Myb
←HEXIM1
←BRD4
←GAPDH

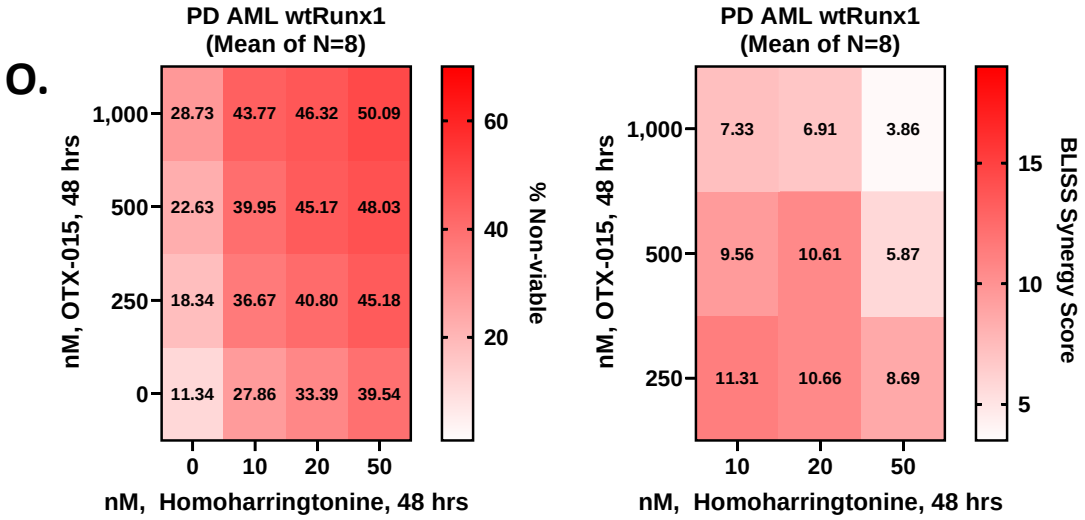
O.
PD AML wtRunx1
(Mean of N=8)
nM, OTX-015, 48 hrs
1,000 28.73 43.77 46.32 50.09
500 22.63 39.95 45.17 48.03
250 18.34 36.67 40.80 45.18
0 11.34 27.86 33.39 39.54
0 10 20 50
nM, Homoharringtonine, 48 hrs
% Non-viable
60
40
20
PD AML wtRunx1
(Mean of N=8)
nM, OTX-015, 48 hrs
1,000 7.33 6.91 3.86
500 9.56 10.61 5.87
250 11.31 10.66 8.69
10 20 50
nM, Homoharringtonine, 48 hrs
BLISS Synergy Score
15
10
5

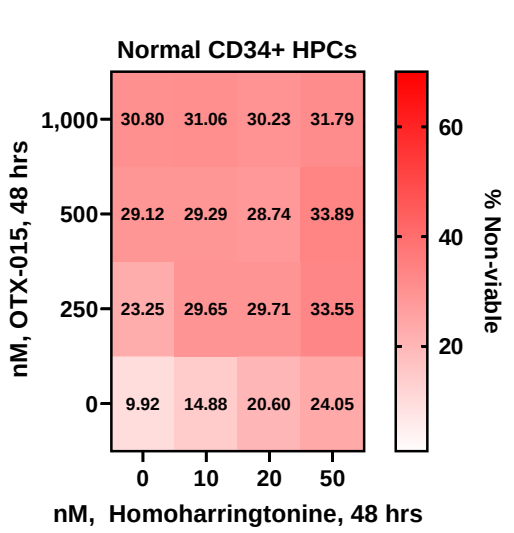
P.
Normal CD34+ HPCs
nM, OTX-015, 48 hrs
1,000 30.80 31.06 30.23 31.79
500 29.12 29.29 28.74 33.89
250 23.25 29.65 29.71 33.55
0 9.92 14.88 20.60 24.05
0 10 20 50
nM, Homoharringtonine, 48 hrs
% Non-viable
60
40
20

Table S1. The RUNX1 mutation(s) identified by NextGen sequencing in the 14 patient-derived mtRUNX1 expressing AML samples utilized in these studies. The nucleotide alteration in the DNA and the resulting protein alteration are shown for each sample.

Patient #	Runx1 Gene Mutation	Runx1 Protein Mutation
1	c. 1281_1285del c. 987_968dupGT c. 900_901insTCCG	p. I428fs*170 p. F330fs*265 p. P301fs*300
2	c. 601 C>T	p. R201*
3	c. 981_982insTCGACCTG	p. T328fs
4	c. 592 G>A	p. D198N
5	c. 238dupG	p. E80fs*58
6	c. 491 T>A c. 485 G>A	p. V164D p. R162K
7	c. 491 T>A c. 485 G>A	p. V164D p. R162K
8	c. 181 G>T	p. E61*
9	c. 596 G>C	p. G199A
10	c. 610 C>T	p. R204*
11	c. 981_982insTCGACCTG	p. T328fs
12	c. 593 A>G c. 592 G>T c. 500 G>A c. 496 C>G	p. D198G p. D198Y p. S167N p. R166G
13	c. 319 C>T c. 737 C>T	p. R107C p. T246M
14	c. 1627 G>T	p. G543C

Fig. S7

A.

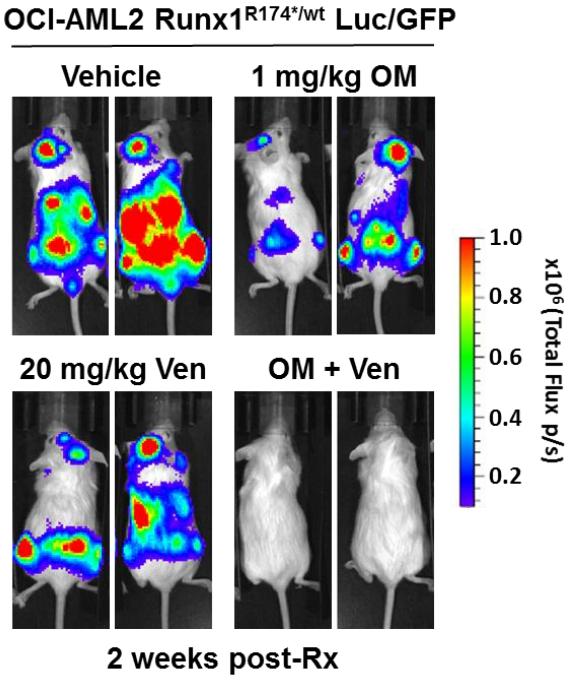

B.

PDX mtRUNX1 AML #8 Cohorts	Median Survival (Days)
Vehicle	49.0
0.5 mg/kg OM	74.5
1.0 mg/kg OM	84.0
20 mg/kg Ven	48.0
30 mg/kg OTX	63.0
1 mg/kg OM & 20 mg/kg Ven	98.5
1 mg/kg OM & 30 mg/kg OTX	102.0

C.

PDX mtRUNX1 AML #8 Comparisons	Significance (Overall Survival, OS)
20 mg/kg Ven vs. 1 mg/kg OM & 20 mg/kg Ven	<0.0001
1 mg/kg OM vs. 1 mg/kg OM & 20 mg/kg Ven	0.0008
30 mg/kg OTX vs. 1 mg/kg OM & 30 mg/kg OTX	0.0003
1 mg/kg OM vs. 1 mg/kg OM & 30 mg/kg OTX	0.0035

Supplemental Materials and Methods:

Contact for Reagent sharing. Kapil N Bhalla. Department of Leukemia, MD. Anderson Cancer Center, 1400 Holcombe Blvd, Unit428, Houston, TX, 77030. kbhalla@mdanderson.org

Reagents and antibodies: Omacetaxine mepesuccinate for in vivo studies was obtained under an MTA from Teva Pharmaceutical (Petah Tikva, Israel). Venetoclax was obtained under an MTA from Abbvie Pharmaceuticals. Homoharringtonine (HHT), OTX015 (BET inhibitor), and Rocaglamide for in vitro studies were obtained from MedChem Express (Monmouth Junction, NJ). Cycloheximide was obtained from Santa Cruz Biotechnology, Inc. (Dallas, TX). All compounds were prepared as 10 mM stocks in 100% DMSO and frozen at -80°C in 5-10 µL aliquots to allow for single use, thus avoiding multiple freeze-thaw cycles that could result in compound decomposition and loss of activity. Anti-pBAD [RRID: AB_560884], anti-BAD [RRID: AB_2062127], anti-Bak [RRID: AB_10828597], anti-Bax [RRID: AB_10557411], anti-BFL-1/A1 [RRID: AB_2798390], anti-BIM [RRID: AB_1030947], anti-CDK4 [RRID: AB_2631166], anti-CEBPα [RRID: AB_11178517], anti-Cleaved PARP [RRID: AB_10699459], anti-c-Myb [RRID: AB_2716637], anti-c-Myc [RRID: AB_1903938], anti-E2F1 [RRID: AB_2096936], anti-GATA2 [RRID: AB_2108579], anti-HEXIM1 [RRID: AB_2797969], anti-MCL-1 [RRID: AB_2799149], anti-p21 [RRID: AB_823586], anti-PU.1 [RRID: AB_10693421], anti-PUMA [RRID: AB_2797920], anti-pRb [RRID: AB_11178658], anti-Rb [RRID: AB_823629], anti-RUNX1/(AML1) [RRID: AB_10859035], anti-RUNX2 [RRID: AB_2732805], anti-RUNX3 [RRID: AB_2798118], anti-p-SAPK/JNK [RRID: AB_2307321], and anti-SAPK/JNK [RRID: AB_2250373] antibodies were obtained from Cell Signaling Technologies (Beverly, MA). Anti-BCL2 [RRID: AB_626733], anti-Bcl-xL [RRID:AB_626739], anti-CDK6 [RRID: AB_10610066], anti-GAPDH [RRID: AB_627679], anti-NOXA [RRID: AB_784877] and anti-β-Actin [RRID: AB_626630] antibodies were obtained from Santa Cruz Biotechnologies (Dallas, TX). Anti-BRD2 [RRID: AB_2034828] and anti-BRD4 [RRID: AB_1576498] antibodies were obtained from Bethyl Labs (Montgomery, TX). Anti-HOXA9 [Cat #: ab140631] and anti-MPL [RRID: AB_10858953] antibodies were obtained from Abcam (Cambridge, MA). Anti-Meis1 [RRID: AB_10983635] antibody was obtained from Thermo Fisher Scientific (Waltham, MA). Anti-p27 [RRID: AB_397637] antibody was obtained from BD Biosciences (San Jose, CA).

Cell lines and cell culture: OCI-AML5 [DSMZ Cat# ACC-247, RRID:CVCL_1620], OCI-AML2 [DSMZ Cat# ACC-99, RRID:CVCL_1619], and Mono-Mac-1 [DSMZ Cat# ACC-252, RRID:CVCL_1425], cells were obtained from the DSMZ. HEK-293T cells were obtained from the Characterized Cell Line Core Facility at M.D. Anderson Cancer Center, Houston TX. All experiments with cell lines were performed within 6 months after thawing or obtaining from ATCC or DSMZ. The

cell lines were also authenticated by STR profiling. OCI-AML2 and OCI-AML5 were cultured in ribonucleoside-containing Alpha-MEM media with 20% FBS, 1% non-essential amino acids (NEAA), and 1% penicillin/streptomycin. Mono-Mac-1 cells were cultured in high-glucose-formulated RPM1 1640 with 20% FBS, 1% NEAA, and 1% penicillin/streptomycin. HEK-293T cells were cultured in high-glucose-formulated DMEM media with 10% FBS, 1% NEAA, 1% L-glutamine, and 1% penicillin/streptomycin. Logarithmically growing, mycoplasma-negative cells were utilized for all experiments. Following drug treatments, cells were washed free of the drug(s) prior to the performance of the studies described.

Cell Line Authentication: The cell lines utilized in these studies were authenticated in the Characterized Cell Line Core Facility at M.D. Anderson Cancer Center, Houston TX utilizing STR profiling.

Generation of Runx1 R174* KI Cell Line Models: The generation of OCI-AML2 Runx1$^{R174*/wt}$ and HL60 Runx1$^{R174*/R174*}$ knock-in models was based on the methods described by Lorenzo Brunetti[1]. To target exon 5 that contains the residue to be mutated (R174), the CHOP-CHOP prediction algorithm[2] was utilized to develop guide RNA. Due to the lower efficiencies, cr-tracrRNA was used over the more commonly utilized sgRNA in order to introduce a break into only one allele. Synthetic crRNA (3 µL of 400 µM stock) was annealed with tracrRNA (1.5 µL of 400 µM stock) at a 2:1 ratio in a 10 µL reaction with 5x annealing buffer via manufacturer's recommended cycling protocol (Synthego, Inc.) in a thermocycler (Bio-Rad T100 thermal cycler). The RNP (ribonucleoprotein complex) for OCI-AML2 cells was generated by incubating 1.6 pmol (3.2 pmol for HL60) of recombinant Cas9 and 7.8 pmol (15.5 pmol for HL60) of cr-tracr RNA for 30 minutes at room temperature. The RNP and dsDNA donor (350 ng) were combined in buffer R and electroporated into 2.5e5 of either OCI-AML2 or HL60 cells utilizing the Neon Transfection System (1600 V, 10 ms, 3 pulses). This was repeated twice (total 5.0e5 cells) and pooled into 2 mL of complete media containing no antibiotics and 2 µM of ROCK inhibitor (Y-27632, Selleck Chemicals; Houston, TX) and allowed to recover. The dsDNA donor contained the truncated Runx1 R174* exon 5, a P2A cleavage site, and the blasticidin resistance gene flanked by two 400-bp homology arms (synthesized by Twist Biosciences). Ten days post-transfection, knock-in cells were selected with the appropriate concentration of Blasticidin (OCI-AML2 15 µg/mL, HL60 4 µg/mL) for 10 days. Following blasticidin selection, the cells were single-cell sorted via flow cytometry into 96-well plates. Clones were expanded and then screened for the knock-in mutation. Genomic DNA was harvested and exon 5 was PCR-amplified with the Sigma Extract-N-Amp Blood PCR kit (XNAB2R-1KT, Sigma-

Aldrich; St. Louis, MO). The PCR product was analyzed for the presence of the R174* mutation via Sanger sequencing (Eurofins Genomics; Louisville, KY).

Primary AML blasts: Patient-derived AML cells samples were obtained with informed consent as part of a clinical protocol approved by the Institutional Review Board of The University of Texas, M.D. Anderson Cancer Center. Normal hematopoietic progenitor cells (HPCs) were obtained from delinked, de-identified cord blood samples. Mononuclear cells were purified by Ficoll Hypaque (Axis Shield, Oslo, Norway) density centrifugation following the manufacturer's protocol. Mononuclear cells were washed once with sterile 1X PBS and suspended in complete RPMI media containing 20% FBS and counted to determine the number of cells isolated prior to immuno-magnetic selection. CD34+ AML blast progenitor cells were purified by immuno-magnetic beads conjugated with anti-CD34 antibody following the manufacturer's protocol (StemCell Technologies, Vancouver, British Columbia) prior to utilization in the cell viability assays, RNA expression, and immunoblot analyses.

Sequencing of primary de novo AML blast cells: We performed targeted next-generation sequencing (NGS) of DNA samples from bone marrow or peripheral blood collected from patients at our center with de novo AML[3]. Diagnostic bone marrow samples were obtained for mutational analysis. Total genomic DNA was extracted from unenriched peripheral blood (PB) or bone marrow (BM) samples using ReliaPrep genomic DNA isolation kit (Promega Corp, Madison, WI, USA). Briefly, a total of 250 ng DNA was utilized to prepare sequencing libraries using Agilent HaloPlex custom Kit (Agilent Technologies, Santa Clara, CA, USA). The entire coding sequences of 81 leukemia-relevant genes were interrogated utilizing a custom-designed next-generation sequencing approach and the Illumina MiSeq platform (Illumina; San Diego, CA, USA; RRID:SCR_016379). The genomic reference sequence used was genome GRch37/hg19. The following software tools were utilized in the experimental setup and data analysis: Illumina Experiment Manager 1.6.0 (Illumina; San Diego, CA, USA), MiSeq Control Software 2.4 (Illumina; San Diego, CA, USA), Real Time Analysis 1.18.54 (Illumina; San Diego, CA, USA), Sequence Analysis Viewer 1.8.37 (Illumina; San Diego, CA, USA), MiSeq Reporter 2.5.1 (Illumina; San Diego, CA, USA), and SureCall 3.0.1.4 (Agilent Technologies; Santa Clara, CA, USA). A minimum of 80% reads at quality scores of AQ30 or higher were required to pass quality control. The lower limit of detection of this assay (analytical sensitivity) for single nucleotide variations was determined to be 5% (one mutant allele in the background of nineteen wild type alleles) to 10% (one mutant allele in the background of nine wild type alleles). Testing of patients with active hematologic malignancies was limited to somatic mutations only.

Analysis of epigenetic state in AML cells *in vitro*. ATAC-Seq analysis of untreated and treated AML cells was performed following a previously described protocol[4]. ATAC-Seq libraries were

generated with a Nextera DNA Library Preparation Kit containing the mutant Tn5 transposase (Illumina, San Diego, CA; Catalog number: FC-121-1030). The DNA fragments were indexed utilizing a Nextera Index Kit (Illumina, San Diego, CA; Catalog number: FC-121-1011) and amplified by PCR utilizing NEBNext® High-Fidelity 2X PCR Master Mix according to the manufacturer's protocol (Cat# M0541; New England Biolabs, Ipswich, MA). Library fragments were amplified for 12 cycles utilizing the denaturation, annealing, and extension times as previously described[4]. The amplified library fragments were PCR-purified with a Qiagen MinElute column (Qiagen, Germantown, MD) then size selected with a 1.0X bead concentration to remove fragments shorter than 200 bp. Library fragments were incubated with AMPure XP SPRI beads (Cat# A63880; Beckman Coulter, Indianapolis, IN) for 10 minutes at room temperature in 1.5 mL microcentrifuge tubes. The mixture was placed on a magnetic stand for 10 minutes. The supernatant was removed and the SPRI beads on the magnet were washed twice with fresh 80% ethanol (30 seconds each wash) and air-dried for 2-3 minutes. Library DNA was eluted from the SPRI beads with a 20 µL volume of 10 mM Tris-HCl (pH 8.5). Beads were incubated at room temperature for 10 minutes, then the tubes were transferred to a magnetic stand for 10 minutes. The supernatant containing the DNA libraries was carefully removed by pipetting and transferred into a clean microcentrifuge tube. The individual libraries were quantified, and quality checked by Thermo Fisher Qubit [Thermo Fisher Qubit fluorimeter, RRID:SCR_018095] fluorometric quantification and Agilent Bioanalyzer 2100 [Agilent 2100 Bioanalyzer Instrument, RRID:SCR_019389] analysis, respectively. Individual libraries were pooled into one tube, purified over a Qiagen MinElute column [QIAGEN, RRID:SCR_008539], eluted in 20 µL of 10 mM Tris, (pH 8.5) and sequenced on a NextSeq 500 next generation sequencer (Illumina NextSeq 500, RRID:SCR_014983) utilizing a 150 cycle mid-output kit (Illumina, San Diego, CA). Raw sequencing data was mapped using Bowtie2[5] [Bowtie 2, RRID:SCR_016368] onto the human genome build UCSC hg38 (NCBI 51) for human data and log2-fold changes were calculated with diffReps[6] [diffReps, RRID:SCR_010873]. Sequence tracks were visualized with IGV software [Integrative Genomics Viewer, RRID:SCR_011793]. We also determined the H3K27Ac status, BRD4, and P300 occupancy in untreated and treated OCI-AML2 $Runx1^{R174*/wt}$ cells by ChIPmentation following a previously described protocol[7], with modifications on the concentration of AmpPure XP beads utilized for dual AmpPure XP SPRI bead selection of the final libraries. We utilized 0.65X beads for the first selection, then a 1.0X bead concentration to narrow the fragment size of the final tagmented ChIP DNA library to between 100 and 250 bp. ChIP input DNA libraries were only selected with a 1.0X bead concentration. The individual libraries (ChIP and input) were quantified and quality-checked with Qubit and Bioanalyzer 2100 analysis, respectively. The libraries were pooled into one tube, purified utilizing a Qiagen MinElute column, and eluted in 20 µL for loading onto a NextSeq500 sequencer utilizing a mid-output or high-output kit kit. Raw sequence data were

mapped to UCSC hg38 (NCBI 51) and log2 fold-changes were calculated with diffReps[6] [diffReps, RRID:SCR_010873]. Sequence tracks were visualized with IGV software[8,9] [RRID:SCR_011793]. To identify super enhancers, we performed a ranked order of super enhancers (ROSE) analysis [ROSE, RRID:SCR_017390] utilizing the H3K27Ac status of the chromatin according to the methods of Loven et al.[10]. Analysis of transcription factor binding motifs in gained ATAC-Seq peaks was performed with HOMER [HOMER, RRID:SCR_010881].

Polysome Profile and Ribo-Lace. Polysome Profiling and Ribo-Lace (analysis of actively translated mRNAs) was performed by Immagina Biotechnology S.r.l. (Trento, Italy). For both profiling and Ribo-Lace, 10 million cells of either OCIAML2 Runx1$^{wt/wt}$ or Runx1$^{R174*/wt}$ were treated for 5 minutes with 10 μg/mL cycloheximide prior to flash-freezing and storage at -80˚C. Ribo-Lace was performed in duplicate. Absorbances were graphed in GraphPad V8 for polysome profiles and area under the curve was calculated with ImageJ software in order to estimate changes in ribosomal subunits (40S, 60S, 80S, polysomes) with the knock-in of a Runx1 mutation.

Transcriptome Analysis. Total RNA was isolated from untreated or homoharringtonine inhibitor-treated AML cells utilizing a PureLink RNA Mini kit from Ambion, Inc. [Ambion Inc., Austin, TX; RRID:SCR_008406]. Sequencing libraries were prepared with ERCC spike-in controls in the MD Anderson Cancer Center DNA Sequencing and Microarray core facility and sequenced on an Illumina HiSeq-4000 next generation sequencer [Illumina HiSeq 3000/HiSeq 4000 System, RRID:SCR_016386]. Each library yielded 30-40 million read pairs. Data was mapped using STAR [STAR; RRID:SCR_004463] and Samtools [SAMTOOLS; RRID:SCR_002105][11,12] onto the human genome build UCSC hg38 (NCBI 51) for human data. Gene expression was assessed using DESeq2[13] [DESeq2, RRID:SCR_015687], then variance stabilization and quantile normalization were applied. We considered that significance was achieved for fold-changes greater than or equal to 1.25X up or down relative to the untreated or parental cells, and p-values less than 0.05. The final p-values were adjusted using the Benjamini & Hochberg method[14]. We inferred enriched pathways using the Gene Set Enrichment (GSEA) method[15], and the gene set collection from the Molecular Signature Database (MSigDB)[16] [Molecular Signatures Database, RRID:SCR_016863].

RNA isolation and quantitative polymerase chain reaction. Following the designated treatments, total RNA was isolated from AML cells utilizing a PureLink RNA Mini kit from Ambion, Inc. (Austin, TX) and reverse transcribed with a High-Capacity Reverse Transcription kit from Life Technologies (Carlsbad, CA). Quantitative real-time PCR analysis for the expression of target genes was performed on cDNA using TaqMan probes and a TaqMan Universal PCR Mastermix (Cat # 4364340; Applied Biosystems Foster City, CA). Relative mRNA expression was normalized to the expression of GAPDH and compared to the untreated cells. Additionally, we probed upstream of protein

synthesis by utilizing a TaqMan array (4414196, ThermoFisher Scientific) in order to determine changes in the levels of tRNA-associated genes.

Detection and quantification of rRNAs in AML cells. The sequences for 5S (NR_023379), 5.8S (NR_003285), 18S (NR_003286), and 28S (NR_003287) rRNAs were obtained from GenBank at NCBI [GenBank, RRID:SCR_002760]. These sequences were utilized for designing qPCR primers with the Primer3 online software tool (http://primer3.ut.ee/)[17] [Primer3, RRID:SCR_003139]. Two non-overlapping primer sets were generated for 18S and 28 rRNA; however due to the size of the rRNA only one primer set was designed to target 5S and 5.8S. Primer sets were tested by qPCR on a StepOnePlus™ Real-Time PCR System [StepOnePlus Real-Time PCR System, RRID:SCR_015805] utilizing SYBR-Green PCR mastermix (Cat # 4309155, Thermo Fisher) and cDNA that had been generated with random hexamers from control and HHT-treated cells. A melt curve analysis was performed to ensure that primer pairs generated only a single product in qPCR. The abundance of rRNA in control and HHT-treated cells from independent experiments was normalized to the expression of β-Actin.

Plasmid Generation, Viral Packaging, and Creation of Cell Lines. Plasmid constructs for the production of lentivirus were transfected with packaging plasmids psPAX2 and pMD2.G into HEK-293T cells utilizing jetPRIME reagent (PolyPlus Transfection, New York, NY). The psPAX2 and pMD2.G packaging plasmids were a gift from Didier Trono (Addgene plasmid #12260 and #12259 [RRID:Addgene_12260; RRID: Addgene_12259]). Media was changed the following day. Viral supernatant was collected 72 hours post transfection and filtered through a 0.45 µm PES membrane. AML cells were seeded at 5 x 10^5 cells/mL in a 50:50 mix of media and lentiviral supernatant and supplemented with 8 µg/mL polybrene (Sigma-Aldrich). The following day, the viral supernatant was removed by centrifugation and cells were transduced with fresh viral supernatant for an additional 24 hours. To generate luciferase-expressing OCI-AML2 Runx1$^{R174*/wt}$ cells, pHIV-Luc-ZsGreen (a gift from Bryan Welm [Addgene plasmid #39196;http://n2t.net/addgene:39196; RRID:Addgene_39196]) was packaged as above and transduced into OCI-AML2 Runx1$^{R174*/wt}$ cells. ZsGreen-positive cells were sorted by flow cytometry (FACSAria, FL-1 channel, top 10% brightest GFP-expressing cells), and expanded in culture prior to their utilization in therapeutic in vivo mouse studies.

Cell cycle analysis of AML cells. OCI-AML2 and OCI-AML2 RUNX1$^{R174*/wt}$ cells were harvested by centrifuging at 125 x g for 5 minutes. Cells were washed twice with 1× phosphate-buffered saline (PBS) in 12 x 75 mm flow tubes, re-suspended in 200 µL of 1X PBS and fixed in 70% ethanol by adding 800 µL of molecular grade 70% ethanol dropwise to the cells in the tube. The tubes were then vortexed to mix and stored overnight at -20°C. Fixed cells were washed twice with 1× PBS by

centrifuging at 125 x g for 5 minutes and then stained in 250 µL of DNA staining buffer [5 mL Triton-PBS (100 µL of Triton X100 in 100 mL of 1X PBS) with 100 µL of 1 mg/mL propidium iodide and 100 µL of 10 mg/mL RNAse A] in the dark for 15 minutes at 37°C. Cell-cycle data were collected on a flow cytometer with an argon-488 nM laser in the FL-2 channel and analyzed with Accuri CFlow6 software (BD Biosciences, San Jose, CA).

Assessment of apoptosis by annexin-V staining. Untreated or drug-treated cells were stained with Annexin-V (Pharmingen, San Diego, CA) and TO-PRO-3 iodide (Life Technologies, Carlsbad, CA) and the percentages of apoptotic cells were determined by flow cytometry. To analyze synergism, cells were treated with combinations for 8, 16, 24, or 48 hours and the percentages of annexin V-positive, apoptotic cells or % PI-positive, non-viable cells were determined by flow cytometry. We utilized matrix dosing of agents in combinations to allow synergy assessment by Bliss scoring utilizing the SynergyFinder V2 online web application tool (http://synergyfinder.fimm.fi/)[18,19].

Assessment of percentage non-viable cells. Following designated treatments, PD AML cells were stained with propidium iodide or TO-PRO-3 iodide (Life Technologies, Carlsbad, CA) and analyzed by flow cytometry on a BD Accuri CFlow-6 flow cytometer (BD Biosciences, San Jose, CA).

Assessment of leukemia cell differentiation. Untreated or treated (DMSO) cells were harvested and washed with 1X PBS. Cells were re-suspended in 0.5% BSA/PBS and stained with FITC-conjugated anti-CD86 antibody [RRID:AB_396012], PE-conjugated anti-CD14 [RRID:AB_395799], APC-conjugated anti-CD11b antibody [RRID:AB_398456], anti-CD117(c-Kit)-APC conjugated antibody (BD Biosciences Cat# 561118, [RRID: AB_10562384], or FITC-conjugated IgG1 isotype control [RRID:AB_396090], PE-conjugated IgG1 isotype control [RRID:AB_395953], or APC-conjugated IgG1 isotype control antibodies [RRID:AB_398613] in the dark, on ice for 30 minutes. Cells were washed with 0.5% BSA/PBS by centrifugation at 125 x g for 5 minutes, and then re-suspended in 0.5% BSA/PBS for analysis by flow cytometry. Cells were assessed in the FL-1 and FL-4 fluorescence channels. Differentiation of leukemia cells was also determined by examination of cellular/nuclear morphology. Cells were cytospun onto glass slides at 500 rpm for 5 minutes. The cytospun cells were fixed and stained with a Protocol® HEMA3 stain set (Fisher Scientific, Kalamazoo, MI). Cellular/nuclear morphology was assessed by light microscopy. Two hundred cells were counted in at least five sections of the slide for each condition. The % morphologic differentiation is reported relative to control cells.

Protein synthesis assay. The quantification of nascent polypeptide elongation inhibition was performed as described by the manufacture (ab239725 Abcam; Cambridge, MA) In brief, OCIAML2 parental and mtRunx1 isogenic cells were treated with varying doses of homoharringtonine (HHT) or 10 μg/mL cycloheximide for 4 hrs. In the last 30 minutes of treatment, cells were incubated in the presence of OP-Puromycin (OPP) which is incorporated into nascent polypeptide chains. The cells were then fixed and permeabilized. Next, via click chemistry, OPP was subsequently labeled with fluorescent azide and inhibition of protein synthesis by HHT was quantified by flow cytometry.

Assessment of BAK conformation change. OCI-AML2 and OCI-AML2 RUNX1$^{R174*/wt}$ cells (250,000) were treated with venetoclax for 16 hrs and then analyzed for Bak activation. Bak conformation was assessed via flow cytometry following the methods of Dewson[20] with the following modifications. Prior to fixation the cells were centrifuged at 125 x g and after at 600 x g. The Bak-NT antibody (RRID:AB_310159) was used at 5 µg/mL. Normal rabbit IgG (RRID:AB_490574) was utilized as a negative control. For flow cytometry analysis, cells were resupended in 100 µL of intracellular FACS buffer. For detection FITC Goat Anti-Rabbit IgG (RRID:AB_395212) was utilized.

scRNA-Seq. PD mtRunx1 AML #11 was treated with 100 nM HHT (2 million cells per condition) for 8 hrs then cryopreserved (10% DMSO/FBS) until processing of sample. The AML sample was processed according to the manufacturer, 10x Genomics, recommendation for scRNA-Seq (Fresh Frozen Human PBMCs for Single Cell RNA Sequencing and Chromium Next GEM Single Cell 3' Reagent Kits v3.1 User Guide). Indexed cDNA libraries were sequenced on a NovaSeq6000 sequencer. Cell clusters were defined by Cell Ranger utilizing standard pipelines and imaged by Loupe Browser software. Composition of cells within each cluster was determined by SingleR algorithm [21]. Differential gene expressions were determined as greater than 1.25-fold up or down and a p-value less than 0.05.

Cell lysis and protein quantitation. Untreated or drug-treated cells were centrifuged, and the cell pellets were incubated in lysis buffer on ice for 20 minutes[22]. After centrifugation, an aliquot of each cell lysate was diluted 1:10 and the protein content was quantitated using a BCA protein quantitation kit (Pierce, Rockford, IL), according to the manufacturer's protocol. Protein concentrations were determined by comparing the absorbance at 562 nm compared to a known concentration range of bovine serum albumin (BSA) from 0.125 mg to 2 mg/mL.

SDS-PAGE and immunoblot analyses. Thirty micrograms of total cell lysate were used for SDS-PAGE. Western blot analyses were performed on total cell lysates using specific antisera or monoclonal antibodies. Blots were washed with 1X Phosphate Buffered Saline with Tween®20 (PBST), then incubated in IRDye 680RD goat anti-mouse (RRID:AB_10956588) or IRDye 800CW goat anti-rabbit (RRID:AB_621843) secondary antibodies (LI-COR, Lincoln, NE) for 1 h, washed three times in 1X PBST and scanned with an Odyssey CLX Infrared Imaging System utilizing Image Studio 5.0 Software (RRID:SCR_015795) (LI-COR, Lincoln, NE). The expression levels of β-Actin or GAPDH in the cell lysates were used as the loading control for the western blots. Immunoblot analyses were performed at least twice. Representative immunoblots were subjected to densitometry analysis. Densitometry analysis was performed using ImageJ software [ImageJ, RRID:SCR_003070] [23].

Single cell next-generation mass cytometry 'CyTOF' analysis of PD CD34+ AML cells. Primary, patient-derived CD34+ AML cells were treated with 20 nM HHT, 100 nM HHT, 50 nM VEN, 100 nM VEN, 1000 nM OTX015, 20nM HHT plus 50 nM VEN, and 20 nM HHT plus 1000 nM OTX015 for 16 hours. At the end of treatment, cells were fixed with 4% paraformaldehyde for 10 minutes, and then permeabilized with methanol. Cells were blocked for 30 minutes and a cocktail of antibodies conjugated to transition element isotopes were used as tags in atomic mass spectrometric analysis of the cells. Time-of-flight mass spectrometry measured multiple different cellular parameters, simultaneously in each cell, as previously described[24]. The changes in the normalized mass cytometry data between untreated and treated cells were analyzed by Astrolabe[25,26]. Our analysis revealed a distinct cluster of cells that varied in the intensity of expression of leukemia stem cell markers including CD117 Hi, CD123 Hi, CD244 Hi, CD86 Lo, and CD11b Lo. Changes in the percentage of stem cells relative to the total cell population determined by Astrolabe as well as absolute fold changes in protein expression in HHT, OTX015 or venetoclax treated cells compared to untreated cells were graphed with Graph Pad V8.

In vivo model of de novo AML: All in vivo studies were approved by and conducted in accordance with the guidelines of the IACUC at the M.D. Anderson Cancer Center, an AAALAC-accredited facility. Female NOD.Cg-Prkdc^{scid} Il2rg^{tm1Wjl}/SzJ (NSG) mice (stock number: 005557; 4-6 weeks of age) [Jackson Labs, Bar Harbor, ME; RRID: IMSR_JAX:005557] were exposed to 2.5 Gy of radiation. The following day, mice (n=10 per cohort) were injected in the lateral tail vein with 2.0 x 10^6 GFP-luciferase expressing OCI-AML2 Runx1$^{R174*/wt}$ cells or a GFP-luciferase expressing DF64519 mtRunx1 AML PDX (from Dana Farber) and monitored for 4-5 days. Mice were imaged utilizing a Xenogen Lumina in vivo imaging system to document engraftment before treatment was

initiated. Mice were randomized into groups based on equivalent mean bioluminescent intensity to control for variation in cell engraftment and variation between different treatment groups. Treatments were initiated on day 8. For the OCI-AML2 model, cohort one mice were treated with 1.0 mg/kg of omacetaxine mepesuccinate daily for 1 week, followed by 3d for 2 weeks by subcutaneous injection. In the second cohort, mice were treated with 20 mg/kg of venetoclax daily for 2 weeks, then the dose was reduced to 10 mg/kg (by oral gavage) for the third week of treatment. The third cohort of mice were treated with 30 mg/kg of OTX015 daily for 3 weeks by oral gavage. In the fourth cohort, mice were treated with omacetaxine mepesuccinate and venetoclax at the dosage and regiment described above. Mice were imaged weekly by bioluminescent imaging to document treatment efficacy and/or disease progression. Total bioluminescence (Flux) was recorded as photons/second. Leukemia reduction significance was determined by a two-tailed, unpaired, t-test. Mice that became moribund or experienced hind limb paralysis were euthanized according to the approved IACUC protocol. Department of Veterinary Medicine staff members assisting in determining when euthanasia was required were blinded to the experimental conditions of the study. The survival of the mice is represented by a Kaplan-Meier plot. Significance was determined by a Mantel-Cox log rank test. P-values of less than 0.05 were assigned significance.

For the DF64519 AML PDX mouse model, the first cohort of mice were treated with 0.5 mg/kg of omacetaxine mepesuccinate daily for 6 weeks by subcutaneous injection. The second cohort of mice were treated with 1.0 mg/kg of omacetaxine mepesuccinate daily for 3 weeks, followed by 3 weeks at 0.5 mg/kg by subcutaneous injection. In the third cohort, mice were treated with 20 mg/kg of venetoclax daily for 6 weeks by oral gavage. The fourth cohort of mice were treated with 30 mg/kg of OTX015 daily for 3 weeks, followed by 3 weeks at 20 mg/kg by oral gavage. In the fifth cohort, mice were treated with 1.0 mg/kg omacetaxine mepesuccinate and 20 mg/kg Venetoclax with the regiment described above. The last cohort of mice were treated with 1.0 mg/kg omacetaxine mepesuccinate and 30 mg/kg OTX015 with the regiment described above. All mice in each treatment cohort were imaged utilizing a Xenogen Lumina in vivo imaging system once per week to monitor disease status and treatment efficacy. Total bioluminescence (Flux) was recorded as photons/second. Mice that became moribund or experienced hind limb paralysis were euthanized according to the approved IACUC protocol. Department of Veterinary Medicine staff members assisting in determining when euthanasia was required were blinded to the experimental conditions of the study. The survival of the mice is represented by a Kaplan-Meier plot. Significance was determined by a Mantel-Cox log rank test. P-values of less than 0.05 were assigned significance.

Power analysis for in vivo studies. With a sample size of 10 mice per group, we can achieve 79.5% power to detect a difference of overall survival at a significance level of 0.05 with one-sided log-rank test, assuming 30% of mouse-survival at the end of study in the experimental group.

Statistical analysis. Significant differences between values obtained in AML cells treated with different experimental conditions compared to untreated control cells were determined using the Student's t-test in GraphPad V8 [GraphPad Prism, RRID:SCR_002798]. For the *in vivo* mouse models, a two-tailed, unpaired t-test was utilized for comparing total bioluminescent flux. For survival analysis, a Kaplan-Meier plot and a Mantel–Cox log rank test were utilized for comparisons of different cohorts. P values of < 0.05 were assigned significance.

Data and Software availability. ATAC-Seq, ChIP-Seq, bulk RNA-Seq, and single cell RNA-Seq datasets have been deposited in GEO and assigned accession IDs: GSE181977 [ATAC-seq], GSE182006 [ChIP-seq], GSE182018 [RNA-seq], GSE182020 [scRNA-seq]. These data are also included within a Super Series assigned accession ID: GSE182023.

REFERENCES for Supplemental Methods

1. Brunetti L, Gundry MC, Sorcini D, et al. Mutant NPM1 Maintains the Leukemic State through HOX Expression. *Cancer Cell*. 2018;34(3):499-512 e499.
2. Labun K, Montague TG, Krause M, Torres Cleuren YN, Tjeldnes H, Valen E. CHOPCHOP v3: expanding the CRISPR web toolbox beyond genome editing. *Nucleic Acids Res*. 2019;47(W1):W171-W174.
3. Khan M, Cortes J, Kadia T, et al. Clinical Outcomes and Co-Occurring Mutations in Patients with RUNX1-Mutated Acute Myeloid Leukemia. *Int J Mol Sci*. 2017;18(8).
4. Buenrostro JD, Wu B, Chang HY, Greenleaf WJ. ATAC-seq: A Method for Assaying Chromatin Accessibility Genome-Wide. *Curr Protoc Mol Biol*. 2015;109:21 29 21-29.
5. Langmead B, Salzberg SL. Fast gapped-read alignment with Bowtie 2. *Nat Methods*. 2012;9(4):357-359.
6. Shen L, Shao NY, Liu X, Maze I, Feng J, Nestler EJ. diffReps: detecting differential chromatin modification sites from ChIP-seq data with biological replicates. *PLoS One*. 2013;8(6):e65598.
7. Schmidl C, Rendeiro AF, Sheffield NC, Bock C. ChIPmentation: fast, robust, low-input ChIP-seq for histones and transcription factors. *Nat Methods*. 2015;12(10):963-965.
8. Robinson JT, Thorvaldsdottir H, Winckler W, et al. Integrative genomics viewer. *Nat Biotechnol*. 2011;29(1):24-26.
9. Thorvaldsdottir H, Robinson JT, Mesirov JP. Integrative Genomics Viewer (IGV): high-performance genomics data visualization and exploration. *Brief Bioinform*. 2013;14(2):178-192.
10. Loven J, Hoke HA, Lin CY, et al. Selective inhibition of tumor oncogenes by disruption of super-enhancers. *Cell*. 2013;153(2):320-334.
11. Dobin A, Davis CA, Schlesinger F, et al. STAR: ultrafast universal RNA-seq aligner. *Bioinformatics*. 2013;29(1):15-21.

12. Li H, Handsaker B, Wysoker A, et al. The Sequence Alignment/Map format and SAMtools. *Bioinformatics*. 2009;25(16):2078-2079.
13. Love MI, Huber W, Anders S. Moderated estimation of fold change and dispersion for RNA-seq data with DESeq2. *Genome Biol*. 2014;15(12):550.
14. Benjamini Y, Hochberg Y. Controlling the False Discovery Rate: A Practical and Powerful Approach to Multiple Testing. *Journal of the Royal Statistical Society: Series B (Methodological)*. 1995;57(1):289-300.
15. Subramanian A, Tamayo P, Mootha VK, et al. Gene set enrichment analysis: a knowledge-based approach for interpreting genome-wide expression profiles. *Proc Natl Acad Sci U S A*. 2005;102(43):15545-15550.
16. Liberzon A, Subramanian A, Pinchback R, Thorvaldsdottir H, Tamayo P, Mesirov JP. Molecular signatures database (MSigDB) 3.0. *Bioinformatics*. 2011;27(12):1739-1740.
17. Untergasser A, Cutcutache I, Koressaar T, et al. Primer3--new capabilities and interfaces. *Nucleic Acids Res*. 2012;40(15):e115.
18. Ianevski A, Giri AK, Aittokallio T. SynergyFinder 2.0: visual analytics of multi-drug combination synergies. *Nucleic Acids Res*. 2020;48(W1):W488-W493.
19. Ianevski A, He L, Aittokallio T, Tang J. SynergyFinder: a web application for analyzing drug combination dose-response matrix data. *Bioinformatics*. 2020;36(8):2645.
20. Dewson G. Detection of Bak/Bax activating conformation change by intracellular flow cytometry. *Cold Spring Harb Protoc*. 2015;2015(5):477-480.
21. Aran D, Looney AP, Liu L, et al. Reference-based analysis of lung single-cell sequencing reveals a transitional profibrotic macrophage. *Nat Immunol*. 2019;20(2):163-172.
22. Fiskus W, Verstovsek S, Manshouri T, et al. Heat shock protein 90 inhibitor is synergistic with JAK2 inhibitor and overcomes resistance to JAK2-TKI in human myeloproliferative neoplasm cells. *Clin Cancer Res*. 2011;17(23):7347-7358.
23. Schneider CA, Rasband WS, Eliceiri KW. NIH Image to ImageJ: 25 years of image analysis. *Nat Methods*. 2012;9(7):671-675.
24. Bendall SC, Simonds EF, Qiu P, et al. Single-cell mass cytometry of differential immune and drug responses across a human hematopoietic continuum. *Science*. 2011;332(6030):687-696.
25. Behbehani GK, Samusik N, Bjornson ZB, Fantl WJ, Medeiros BC, Nolan GP. Mass Cytometric Functional Profiling of Acute Myeloid Leukemia Defines Cell-Cycle and Immunophenotypic Properties That Correlate with Known Responses to Therapy. *Cancer Discov*. 2015;5(9):988-1003.
26. Gottfried-Blackmore A, Rubin SJS, Bai L, et al. Effects of processing conditions on stability of immune analytes in human blood. *Sci Rep*. 2020;10(1):17328.